

**The effects of microRNA-19b overexpression and knockdown
in the basolateral amygdaloid nucleus on noradrenergic
metabolism**

Brandon K. K. Fields

Undergraduate thesis submitted to the Department of Integrative
Physiology

University of Colorado Boulder

Defended April 4, 2014

Thesis Advisor

Dr. Christopher A. Lowry, Department of Integrative Physiology and the
Center for Neuroscience

Committee Members

Dr. David Sherwood, Department of Integrative Physiology

Dr. Robert Spencer, Department of Psychology and Neuroscience

Abstract

Stressful events have been shown to increase noradrenergic signaling in key limbic areas, such as the hypothalamus, the amygdala, and the locus coeruleus. The basolateral amygdaloid nucleus (BL) is known to play a central role in the mediation of fear and anxiety responses to potentially harmful stimuli. In order to study the effects of altered noradrenergic signaling in the BL on downstream projection targets, we preferentially overexpressed or knocked-down transcription of microRNA-19b (miR-19b) in order to selectively alter the expression of the β_1 -adrenergic receptor (Adrb1) in the BL of mice. Lentiviral constructs were injected directly into the BL of experimental subjects using stereotaxic surgery, after which mice underwent behavioral testing to assess for anxiety- and fear-like behavior. Mice were sacrificed 52 days following infection with lentiviral vectors. Key brain areas downstream of the BL were microdissected and analyzed using high performance liquid chromatography with electrochemical detection for norepinephrine and 3-methoxy-4-hydroxyphenylglycol concentrations. We observed altered noradrenergic metabolism in brain structures intimately involved in the regulation of anxiety and fear responses, such as the hippocampus and the hypothalamus. Briefly, we saw decreases in noradrenergic metabolism in the paraventricular nucleus of the hypothalamus and the dorsal hippocampus for miR-19b OE, and conversely, increases in noradrenergic metabolism in these same brain regions for miR-19b KD. These data suggest that miR-19b, acting within the BL to modulate Adrb1 expression, can alter noradrenergic metabolism in downstream limbic structures, likely by affecting presynaptic modulation of glutamatergic outputs from the BL to target structures. Our data will hopefully guide further study into noradrenergic limbic circuitry, and thus may provide a deeper understanding of anxiety and affective disorders that plague today's society.

Contributions

Of the work conducted at Dr. Christopher Lowry's Behavioral Neuroendocrinology Laboratory at the University of Colorado Boulder, Boulder, Colorado (see Materials and Methods, sections 2.6-2.7), I assisted in the brain sectioning, the preparation and analysis of microdissected samples via high performance liquid chromatography with electrochemical detection (HPLC-ED) analysis for norepinephrine (NE) and a metabolite of NE degradation, 3-methoxy-4-hydroxyphenylglycol (MHPG), statistical analyses, and generation of figures for both microRNA-19b overexpression (miR-19b OE) and microRNA-19b knockdown (miR-19b KD) experiments. In short, the only portions of the experiments that were conducted in Boulder, Colorado, that I did not assist with were the microdissections of individual brain nuclei.

1. Introduction

The basolateral amygdaloid nucleus (BL) is a key nucleus of the central noradrenergic system that is intimately involved in limbic system mediation of fear and anxiety responses to potentially harmful stimuli (Damasio, 1998; LeDoux, 1998). Stressful events are known to cause a marked increase in NE release in the amygdala as well as the locus coeruleus (LC; Tanaka et al., 2000), which provides the primary noradrenergic input to the BL (Asan, 1998). It has been theorized that these structures, along with the hypothalamus and other intermediary structures, play a key role in the provocation and attenuation of anxiety and/or fear responses, such as the provocation of negative emotions, which are mediated by the central noradrenergic system of the brain (Tanaka et al., 2000). Dysfunction of anxiety and fear circuitry occurs when the response elicited exceeds that which is warranted by the given situation, and/or begins to occur in inappropriate situations (LeDoux 1998), manifesting in the form of a fear or anxiety disorder (e.g. Marks 1987, Öhman 1992). The mechanisms underlying animal models of fear and anxiety, such as classical (Pavlovian) fear conditioning, are thought to have much in common with human anxiety disorders, and are thus extremely valuable in the study of the etiology of human anxiety and affective disorders (Bouton et al., 2001; Pitman et al., 1999; Sullivan et al., 2003).

The LC, in accordance with the classification proposed by Dahlström and Fuxe (1964), has been given the designation of noradrenergic cell group A6, and is the largest noradrenergic nucleus of the central noradrenergic system. The LC has been shown to have prominent roles in numerous regulatory systems in the brain, such as those that promote wakefulness and arousal (Szabadi et al., 2013); as previously noted, of particular interest to this thesis are the dense noradrenergic projections that the LC sends to the BL (Fallon et al., 1978; Jones and

Moore, 1977), by which the LC is thought to play a key role in the regulation of anxiety-like behavior and in the consolidation of fear memory through the activation of β -adrenoreceptors in the BL (Silberman et al., 2012; Qu et al., 2008), which respond in an excitatory fashion to noradrenergic stimulation from the LC (Buffalari and Grace, 2007). Furthermore, noradrenergic innervations of the BL by the LC have also been implicated in the formation and retrieval of emotional memories (Chen and Sara, 2007; Sterpenich et al., 2006).

In order to study the role of noradrenergic input to the BL on noradrenergic transmission in downstream limbic circuitry, we chose to preferentially modulate the expression of the β_1 adrenergic receptor (*Adrb1*) in the BL by altering the transcription of miR-19b specifically in this brain region only. The *Adrb1* is a G_s protein-coupled receptor that, upon stimulation, acts to directly activate adenylyl cyclase in order to stimulate an increase in intracellular cyclic adenosine monophosphate levels (Johnson, 1998; Rosebloom and Klein, 1995), and has been shown to play a central role in the mediation of anxiety-like behavioral responses following fear conditioning (Fu et al., 2008). MicroRNA's are endogenous, single-stranded RNA molecules around 22 nucleotides in length that act to regulate gene expression by binding to messenger RNA's of protein coding genes, resulting in either inhibition of translation, degradation via deadenylation, or both (Henshall 2013). Unpublished data from the laboratory of Dr. Alon Chen indicate that miR-19b in particular targets the *Adrb1* to reduce its expression following activation by association with the argonaute RNA-induced silencing complex catalytic component 2 (*Ago2*). In two following experiments, we either overexpressed or knocked-down miR-19b transcription via the introduction of transgenic lentiviral constructs into the BL of mice. It has been shown that glutamatergic projection neurons from the BL to downstream limbic targets act presynaptically to modulate NE release in target regions (Russell and Wiggins, 2000; Howells and Russell, 2008; Dazzi et al., 2011), and that these glutamatergic projection neurons respond in an excitatory fashion to *Adrb1* stimulation (Buffalari and Grace, 2007; Gean et al., 1992; Huang et al., 1996; Ferry et al., 1997). Thus, we expected to see altered NE metabolism, as quantified both by MHPG concentrations and MHPG:NE ratios, in downstream BL projection targets.

2. Materials and Methods

The overall experimental design is illustrated in Figure 1. Timeline events were identical for both miR-19b OE and miR-19b KD experiments.

Sections 2.1-2.5 pertain to work conducted at Dr. Alon Chen's Neurobiology of Stress Laboratory in Rehovot, Israel. Following brain extractions, brain tissue was transported to Dr.

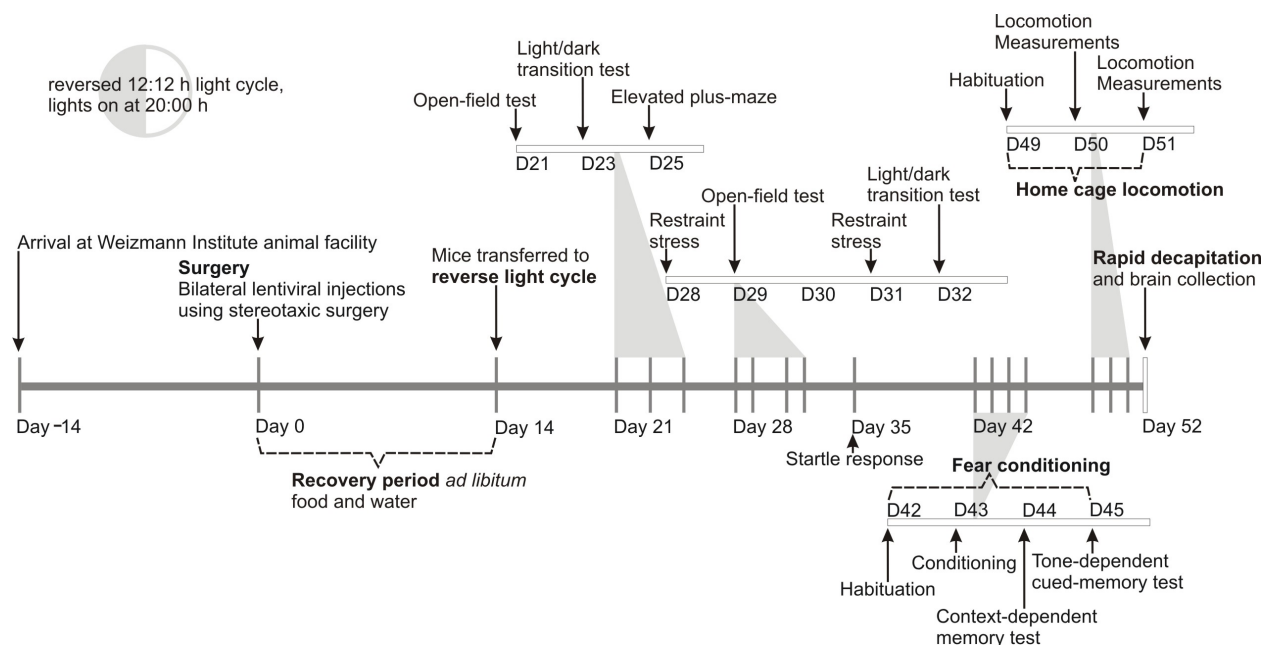


Fig. 1. Timeline of experimental procedures conducted in the laboratory of Dr. Alon Chen at the Weizmann Institute of Science in Rehovot, Israel, for both miR-19b OE and miR-19b KD experiments.

Christopher Lowry's Behavioral Neuroendocrinology Laboratory at the University of Colorado Boulder, Boulder, Colorado, where all following laboratory work and analyses were conducted (sections 2.6-2.7).

2.1. Subjects

C57BL/6J mice (Harlan) were maintained in a pathogen-free temperature-controlled (22 ± 1 °C) mouse facility on a reversed 12-hour light-dark cycle at the Weizmann Institute of Science according to institutional guidelines, with lights on at 20:00 hours. Food (Harlan) and water were given *ad libitum*. The total number of animals used for the lentivirus-injected mice in *Experiment 1* (miR-19b OE experiment) was 20 (10 control and 10 miR-19b OE). The total number of animals used for the lentivirus-injected mice in *Experiment 2* (miR-19b KD experiment) was 24 (12 control and 12 miR-19b KD).

2.2. Lentiviral vectors, infection and expression

The miR-19b overexpression vector was cloned as follows: the enhanced form of human synapsin 1 promoter (Hioki et al., 2007) was PCR amplified (forward primer: tttttatcgatctcgagtagttattaatagtaac, reverse primer: tttttaccggtggcgcgcccgccgcagcgcagatggt) from pENTR1A-E/SYN-GFP-WRPE1 (kindly provided by Dr. Takeshi Kaneko, Department of Morphological Brain Science, Graduate School of Medicine, Kyoto University, Kyoto, Japan)

and inserted between *Clal* and *Agel* restriction sites to replace the CMV promoter in pCSC-SP-PW-IRES/GFP (kindly provided by Dr. Inder Verma, The Salk Institute for Biological Studies, La Jolla, CA). The purpose of replacing the CMV promoter with the synapsin 1 promoter was to ensure a targeted transgenic response, as the human synapsin 1 promoter tends to confer more neuron-specific transgenic expression than the CMV promoter; the CMV promoter tends to mediate transgene expression in glial cells rather than neuronal cells, as evidenced by research conducted with adenoviral vectors (Kügler et al., 2003). The miR19b-EGFP sequence was cut from a *pEGFP-N1-miR-19b* plasmid and ligated to pCSC-Esyn-IRES/GFP using *BamHI* and *BsrGI* replacing the original IRES/GFP sequence (as a control EGFP was cut from pEGFP-N1 using *BamHI* and *BsrGI* to replace IRES/GFP sequence). Green fluorescent protein (GFP) viral constructs were kindly provided by Dr. Inder Verma, The Salk Institute for Biological Studies, La Jolla, CA.

High titer lentiviruses were produced as described previously (Tiscornia et al., 2006). Briefly, recombinant lentiviruses were produced by transient transfection in HEK293T cells. Infectious particles were harvested at 48 and 72 hours post-transfection, filtered through 0.45 µm-pore cellulose acetate filters, concentrated by ultracentrifugation, re-dissolved in sterile Hank's Balanced Salt Solution (HBSS), aliquoted and stored at -80 °C.

The miR-19b KD construct is proprietary to the Chen lab and therefore is not described here.

The control virus used for the miR-19b OE experiment was pcsc-ESYN-GFP. This viral construct utilized an identical vector as the miR-19b OE construct, though it only expressed GFP. The control virus used for the miR-19b KD experiment was p156-pRRL-H1-scramblemiR-CMV-GFP. This viral construct utilized an identical vector as the miR-19b KD virus, though it expressed a scramble instead of the miR-19b KD virus; note that this virus also expressed GFP.

2.3. Stereotactic intracranial injections

A computer-guided stereotaxic instrument and a motorized nanoinjector (Angle Two™ Stereotaxic Instrument, myNeuroLab) were used. Mice were anesthetized using 1.5% isoflurane and 1 µl of the lentiviral preparation was delivered to each BL using a Hamilton syringe connected to a motorized nanoinjector system at a rate of 0.2 µl per minute (coordinates relative to bregma: AP = -1.58 mm, L = ±3.3 mm, H = -4.6 mm). Mice were subjected to behavioral studies following a two-week recovery period.

2.4. Behavioral assessments

All behavioral assessments were performed during the dark phase following habituation to the test room for 2 hours before each test. Behavioral tests were conducted in the following order, from the least stressful paradigm to the most, and ending with locomotor testing: open-field, light/dark transition test, elevated plus-maze, startle response, fear conditioning, and home cage locomotion. All following time points refer to days following stereotactic intracranial injections: open-field testing was conducted first on day 21, and again on day 28 following restraint stress that was administered one day prior. Light/dark transition testing was conducted first on day 25 and again on day 32 following restraint stress that was administered one day prior. Elevated plus-maze testing was conducted on day 25. Baseline startle response was assessed on day 35. The fear conditioning study occurred from days 42-45, with habituation beginning on day 42. Home cage locomotion was assessed on days 49-51, and animals were sacrificed 24 hours following the completion of behavioral testing on day 52 (Fig. 1).

2.4.1. Open-field test

The open-field test was performed in a 50 cm x 50 cm x 22 cm white box, lit to 120 lux. The mice were placed in the box for 10 minutes. Locomotion in the box was quantified using a video tracking system (VideoMot2; TSE Systems, Bad Hamburg, Germany).

2.4.2. Light/dark transition test

The light/dark transition test apparatus consisted of a polyvinyl chloride box divided into a black dark compartment (14 cm x 27 cm x 26 cm) and a connected white 1200 lux illuminated light compartment (30 cm x 27 cm x 26 cm). During the 5-minute test, time spent in the light compartment, distance traveled in light, and number of light-dark transitions were quantified with a video tracking system (VideoMot2; TSE Systems, Bad Hamburg, Germany).

2.4.3. Elevated plus-maze

The apparatus in this test was designed as a plus sign and contained 2 barrier walls and 2 open arms. During the 5-minute test, which was performed in relative darkness (6 lux), the number of entries, distance traveled, and the time spent in the open arms were automatically scored using a video tracking system (VideoMot2, TSE Systems).

2.4.4. Fear Conditioning

A computer-controlled fear conditioning system (TSE Systems) monitored the procedure while measuring freezing behavior (defined as lack of movement except for respiration). On the

first day, mice were habituated for 5 minutes to the fear conditioning chamber, a clear Plexiglas® cage (21 cm × 20 cm × 36 cm) with a stainless steel floor grid within a constantly illuminated (250 lux) fear conditioning housing. Conditioning took place on day 2 in one 5-minute training session. Mice initially explored the context for 2 minutes. Thereafter, two pairings of a co-terminating tone [conditioned stimulus (CS) (Takacs et al., 2010): 30 s, 3,000 Hz, pulsed 10 Hz, 80 dB] and shock [unconditioned stimulus (US): 0.7 mA, 2 s, constant current] with a fixed intertrial interval (ITI) of 60 s were presented. The US was delivered through the metal grid floor. Mice were removed from this chamber 1 minute after the last CS–US pairing. The chamber was cleaned thoroughly with 10% ethanol before each session. The ventilating fan of the conditioning box housing provided a constant auditory background noise [white noise, 62 dB]. Context dependent memory was tested 24 hours after the conditioning by re-exposure to the conditioning box for 5 minutes without any stimuli. The tone-dependent cued-memory test was performed 1 day after the contextual memory test in a novel context: the walls and floor of the box were opaque black Plexiglas® (dimensions were similar to the conditioning box), and the apparatus house-lights and ventilating fan were turned off. Behavior was monitored for 2 minutes without any stimulus before the CS (tone) presentations; thereafter two CS's were presented, separated by a fixed 1-minute ITI. Mice were removed from this box 1 minute after the last CS.

2.4.5. Startle

Startle response (TSE Systems) protocol was adapted from Neufeld-Cohen et al. (2010). Briefly, mice were placed in a small Plexiglas® and wire mesh cage on top of a vibration-sensitive platform in a sound-attenuated, ventilated chamber. A high-precision sensor, integrated into the measuring platform, detected movement. Two high-frequency loudspeakers inside the chamber produced all the audio stimuli. Startle amplitude and latency to peak startle amplitude were measured in response to startle stimuli.

2.4.6. Home cage locomotion

Home cage locomotion was assessed using the InfraMot system (TSE Systems). Mice were housed individually for 72 hours, in which the first 24 hours were considered habituation to the individual housing conditions. Measurements of general locomotion consisted of two light and two dark cycles in the last 48 hours collected at 10-minute intervals.

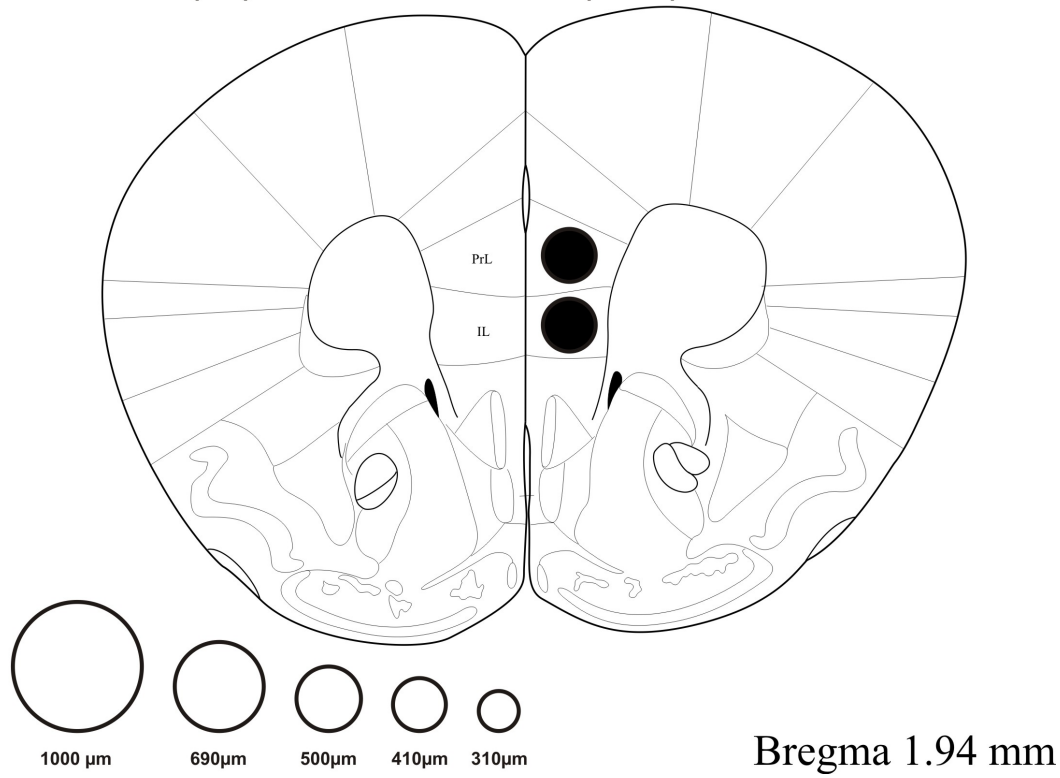
2.5. Brain Extractions

Mice were sacrificed via rapid decapitation on Day 52, and brains were collected for neurochemical analysis.

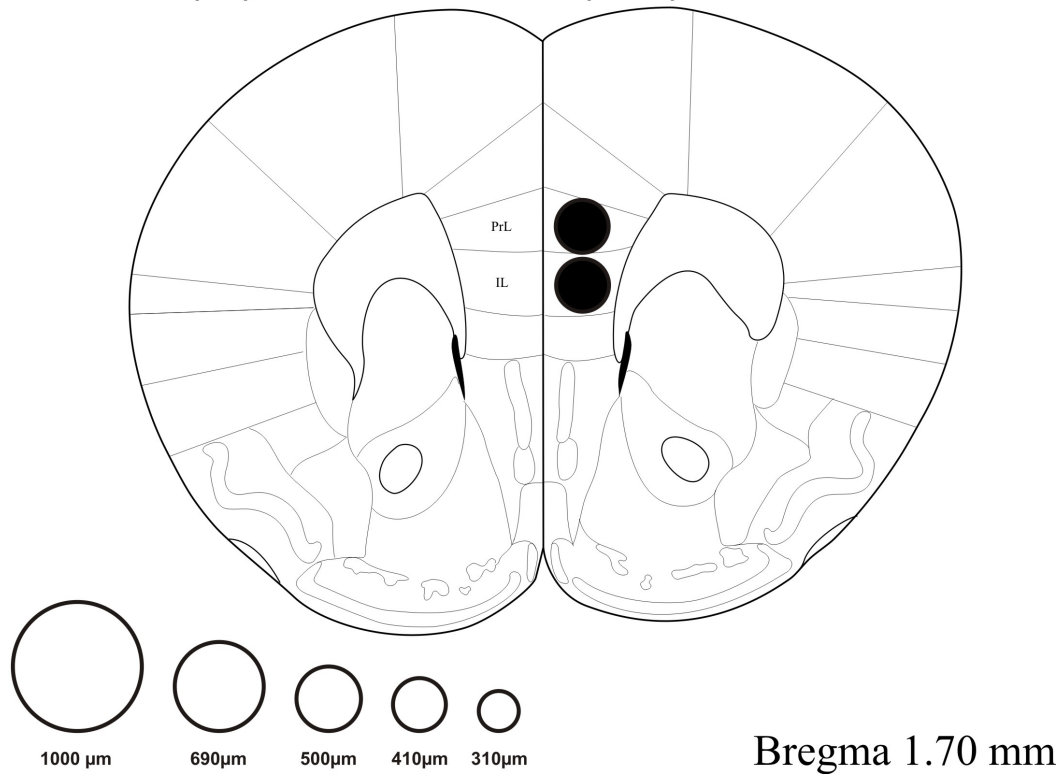
2.6. Microdissections, sample preparation and HPLC-ED analysis of NE and MHPG concentrations

Microdissections were performed as previously described (Palkovits and Brownstein, 1988; Evans et al., 2008). Briefly, coronal brain sections (300 μm) were taken using a precision cryostat (Leica CM1900, North Central Instruments, Plymouth, MN, USA), mounted onto glass slides and microdissected on a cold plate at $-10\text{ }^{\circ}\text{C}$ under a stereomicroscope using microdissection needles with varying inner diameters (Fig. 2). Each microdissected brain structure for each subject was put into separate individual tubes each containing 100 μL of acetate buffer (3.0 g/L sodium acetate, 4.3 mL/L glacial acetic acid; pH adjusted to 5.0), which were rapidly frozen on dry ice and stored at $-80\text{ }^{\circ}\text{C}$. Next, samples were thawed and then centrifuged at $4\text{ }^{\circ}\text{C}$ and 13,000 rpm for 3 minutes. The supernatant was aspirated and 50 μL of the supernatant was used for detection of NE and MHPG using high performance liquid chromatography with electrochemical detection; high performance liquid chromatography with electrochemical detection was performed as described previously (Heal et al., 1989; Evans et al., 2008), but with slight modifications. The pellet was reconstituted with 175 μL of 0.2 M NaOH for later assay of protein content (Pierce Protein Microassay Protocol, Perbio Science UK Ltd., Cramlington, UK). Samples were placed in an ESA model 542 autosampler (ESA, Chelmsford, MA, USA) to automatically inject the samples into the HPLC system. The HPLC system also consisted of an ESA Model 582 Solvent Delivery Module to pump the mobile phase (0.1 M sodium acetate/citric acid buffer dissolved in HPLC grade H_2O , pH = 4.40 adjusted with semiconductor grade NaOH, containing 8% HPLC grade methanol (v/v), and 4.6 mM octanesulphonic acid) through the chromatographic system. The stationary phase, where chromatographic separation occurred, consisted of an integrated pre-column/column system (Ultrasphere 5 ODS (C18) pre-column (45 x 4.6 mm)/Ultrasphere 5 ODS (C18) column (250 x 4.6 mm); MAC-MOD Analytical, USA) maintained at room temperature. Electrochemical detection was accomplished using an ESA Model 5200A Coulochem II detector with dual potentiostats connected to an ESA 5021 Conditioning Cell with the electrode potential set at 0 mV and an ESA 5014B Microdialysis Cell with the channel 1 and channel 2 electrode potentials set at -200 mV and 400 mV , respectively. For each run, the average peak heights of known concentrations of NE and MHPG were determined manually using chromatography analysis software (EZChrom Elite for Windows, Version 2.8; Agilent Technologies, USA) and used to

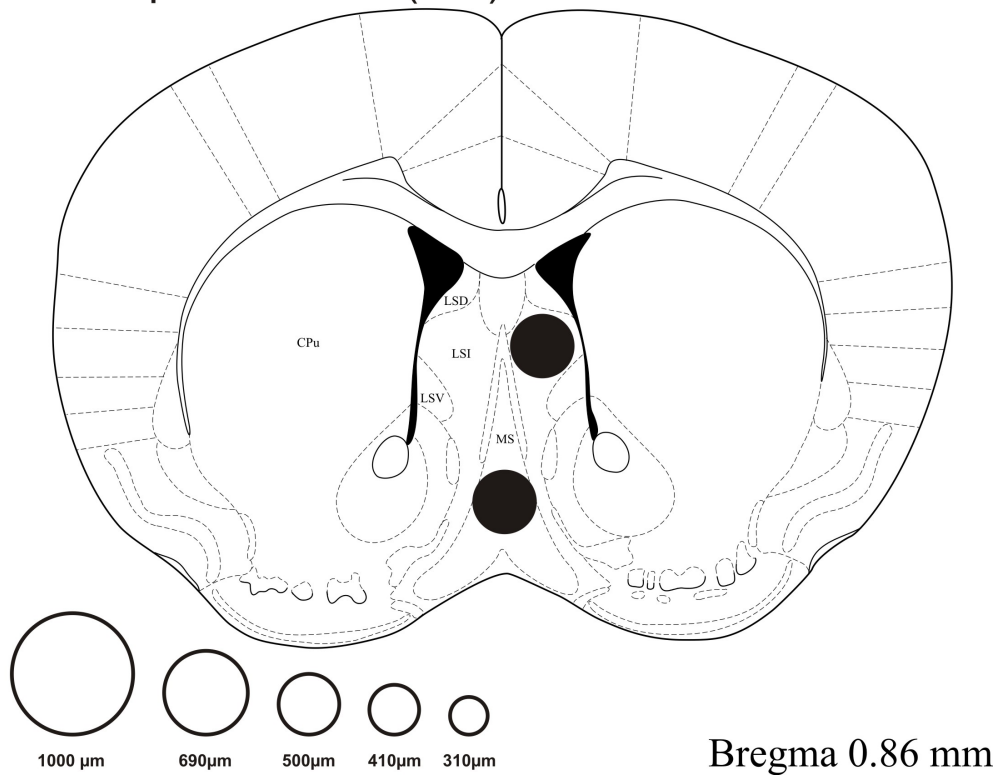
Infralimbic (IL) and Prelimbic (PrL) cortices



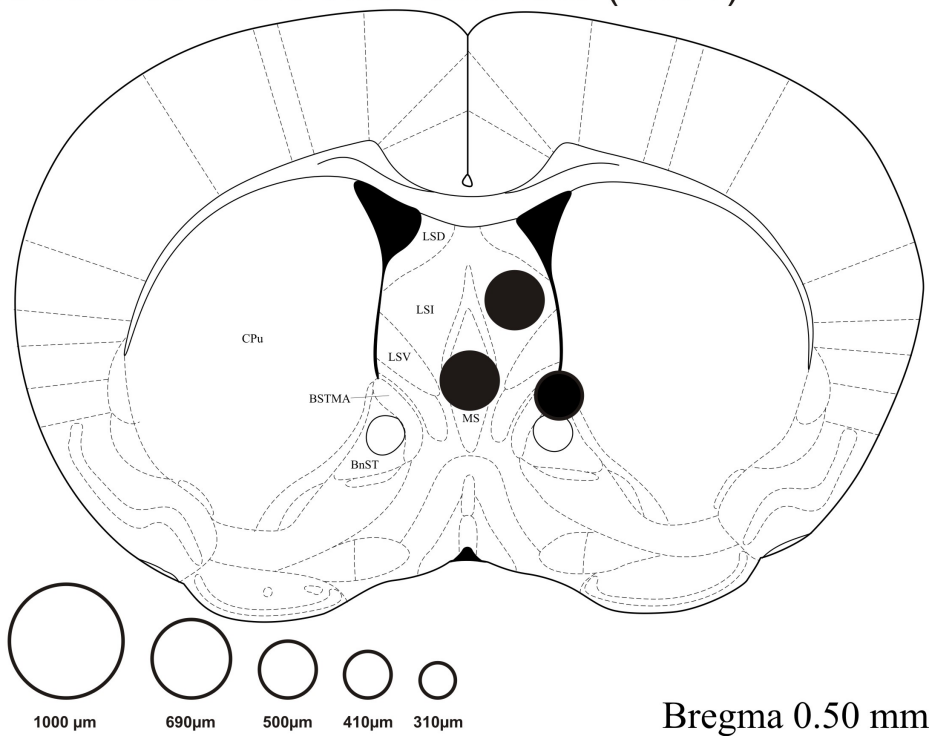
Infralimbic (IL) and Prelimbic (PrL) cortices



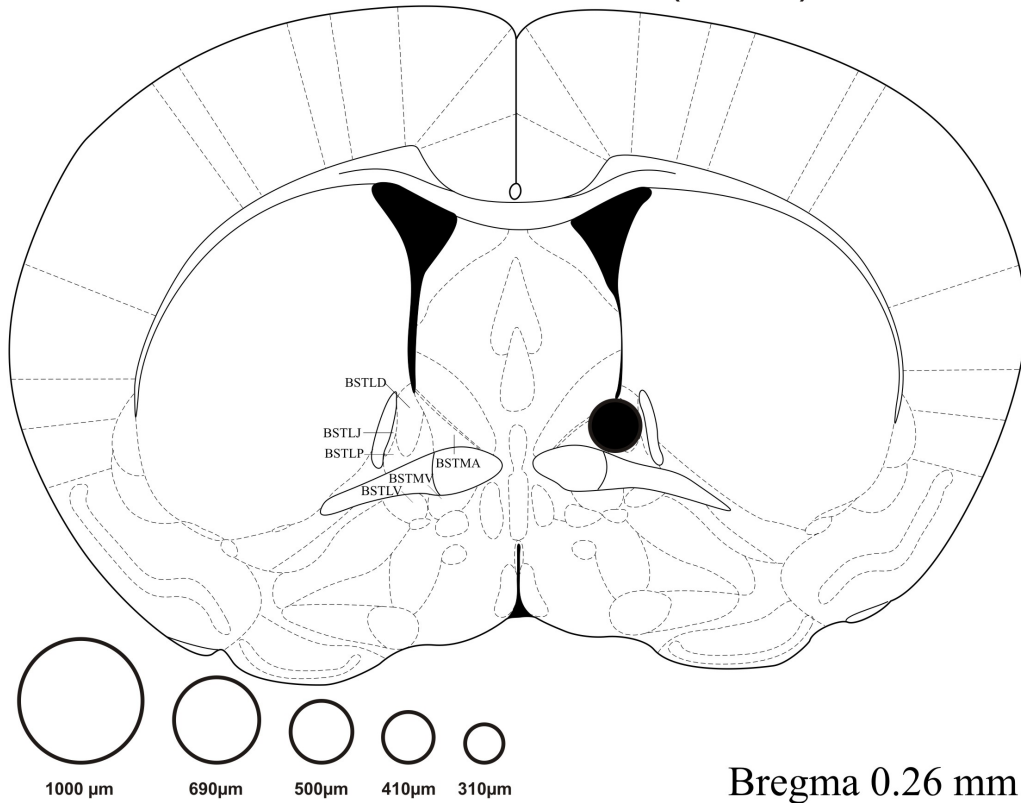
Lateral septal nucleus, intermediate part (LSI) and Medial septal nucleus (MS)



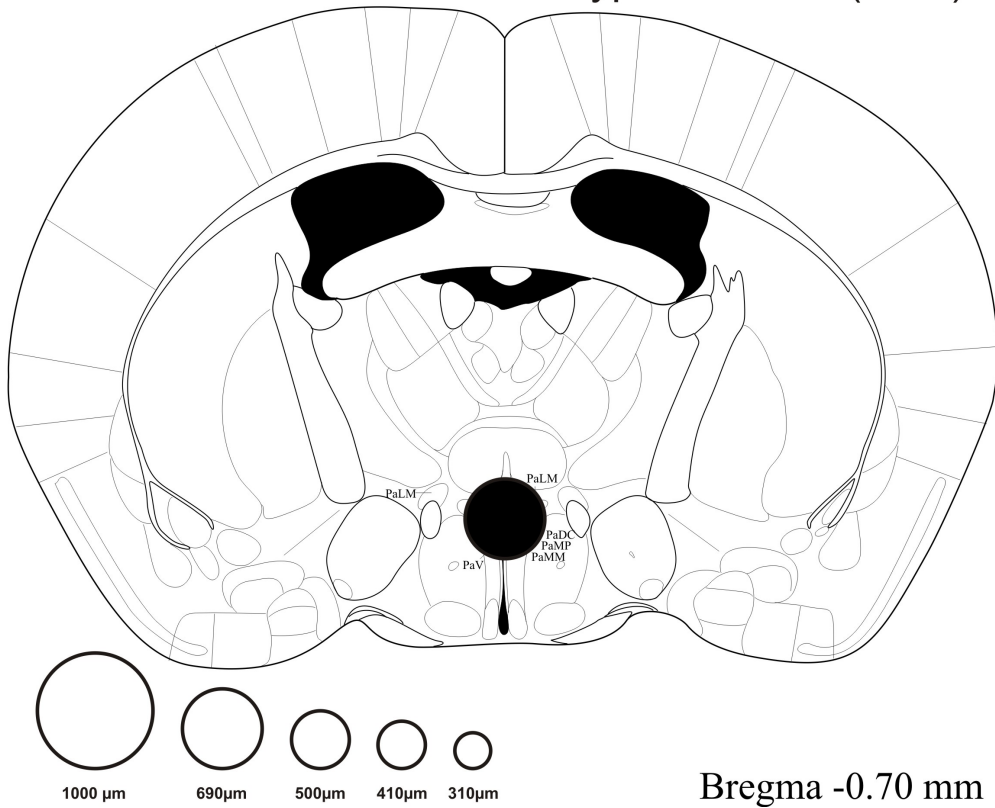
Lateral septal nucleus, intermediate part (LSI), Medial septal nucleus (MS) and Bed nucleus of the stria terminalis (BnST)



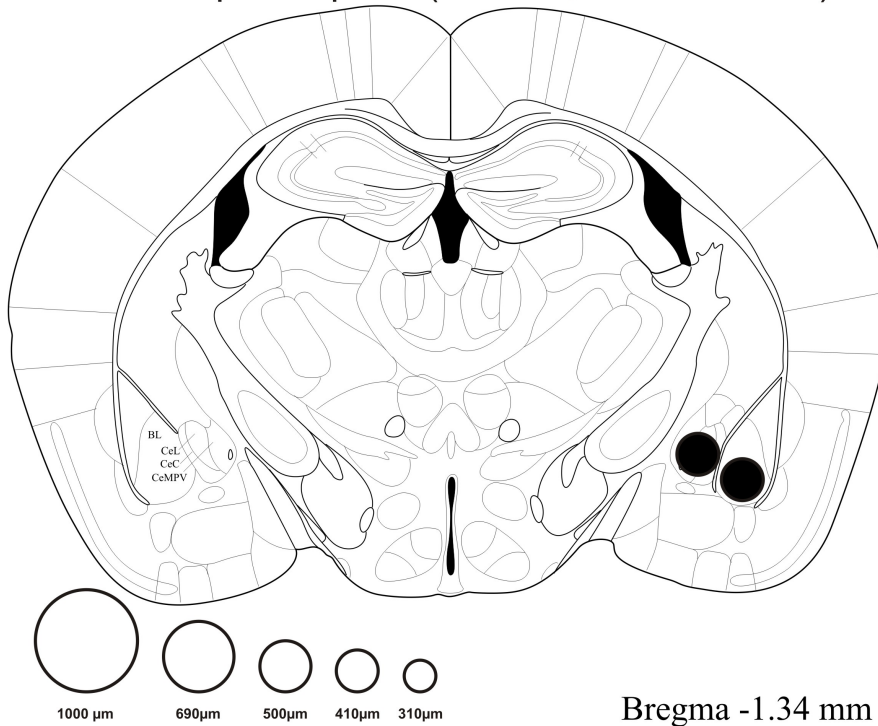
Bed nucleus of the stria terminalis (BnST)



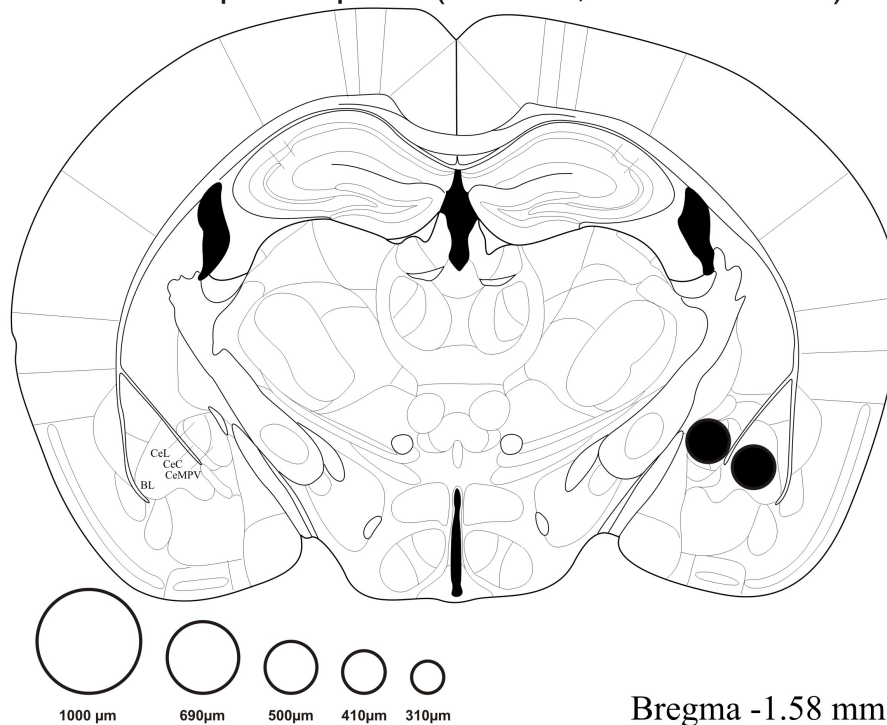
Paraventricular nucleus of the hypothalamus (PVN)



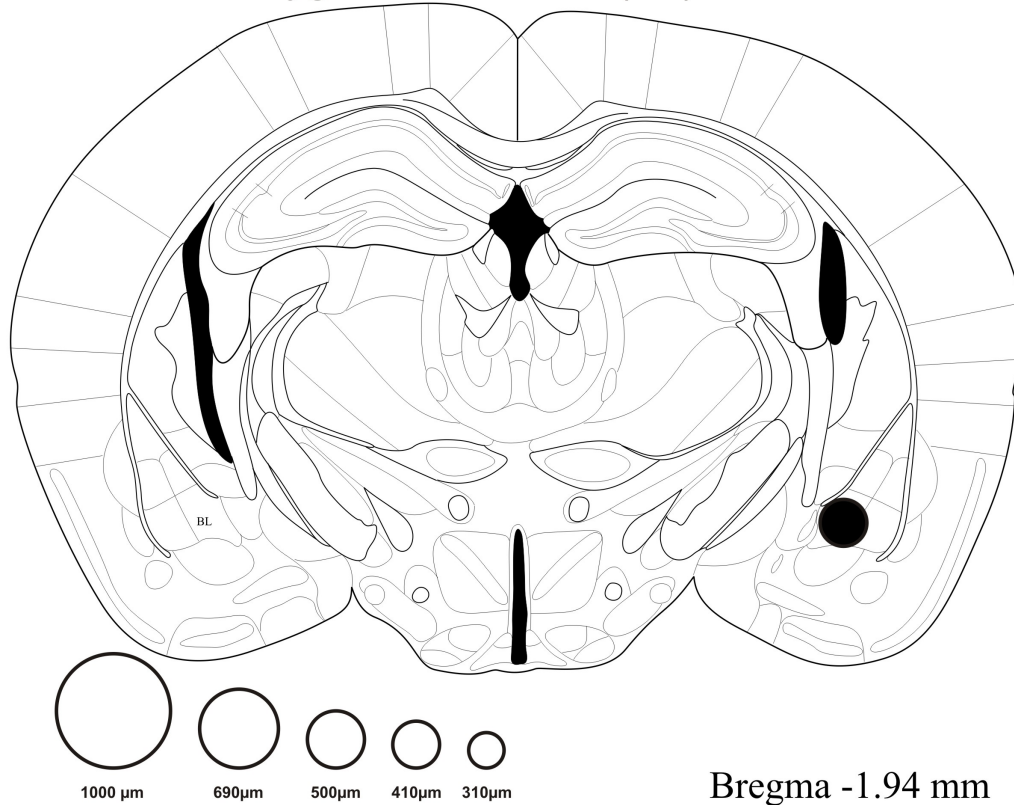
Basolateral amygdaloid nucleus (BL) and
 Central amygdaloid nucleus, medial posteroventral,
 lateral and capsular parts (CeMPV, CeL and CeC)



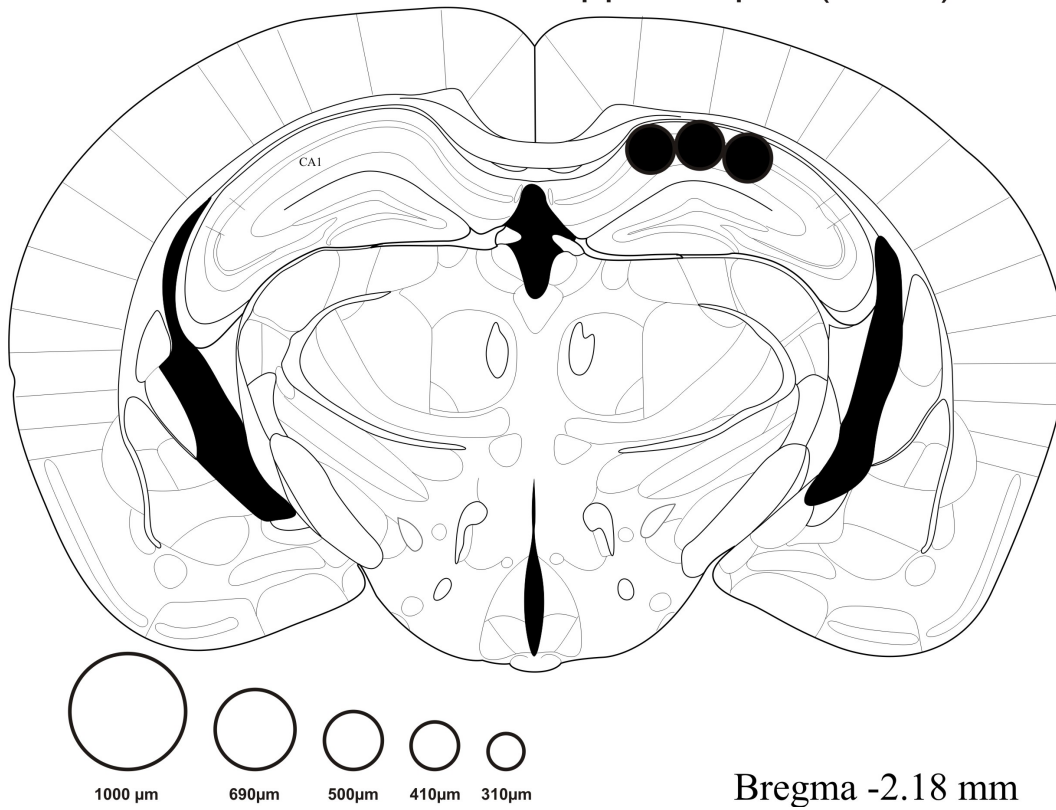
Basolateral amygdaloid nucleus (BL) and
 Central amygdaloid nucleus, medial posteroventral,
 lateral and capsular parts (CeMPV, CeL and CeC)



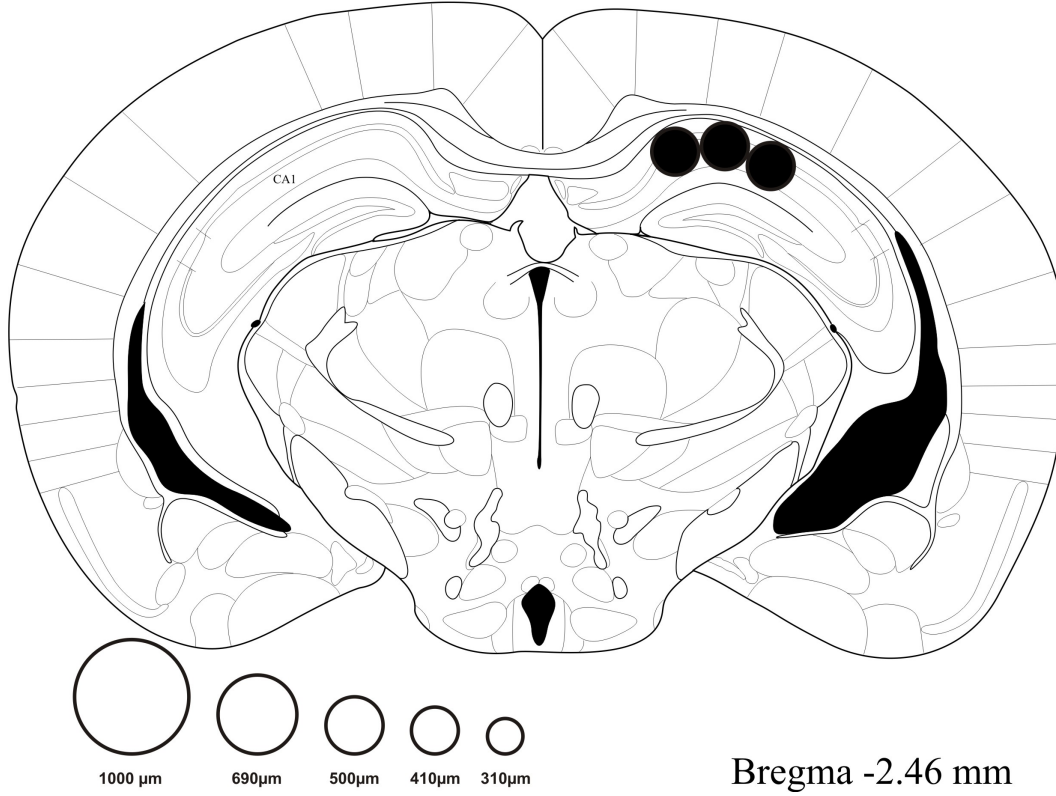
Basolateral amygdaloid nucleus (BL)



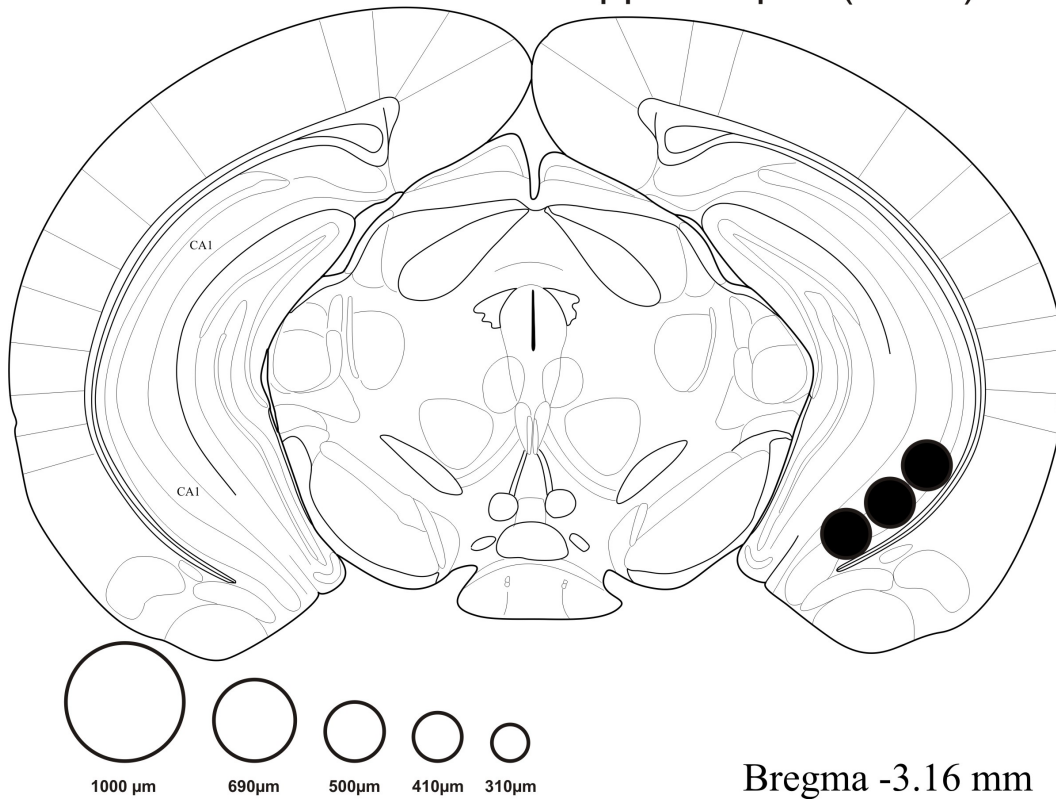
Cornu ammonis 1 of dorsal hippocampus (CA1d)



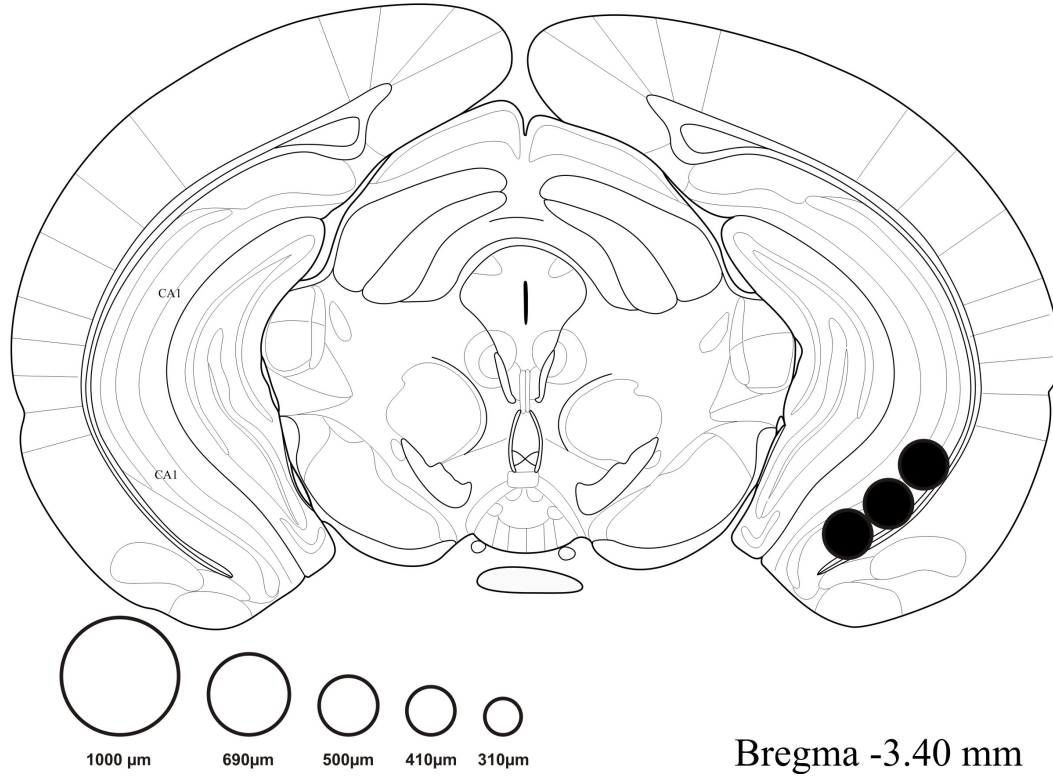
Cornu ammonis 1 of dorsal hippocampus (CA1d)



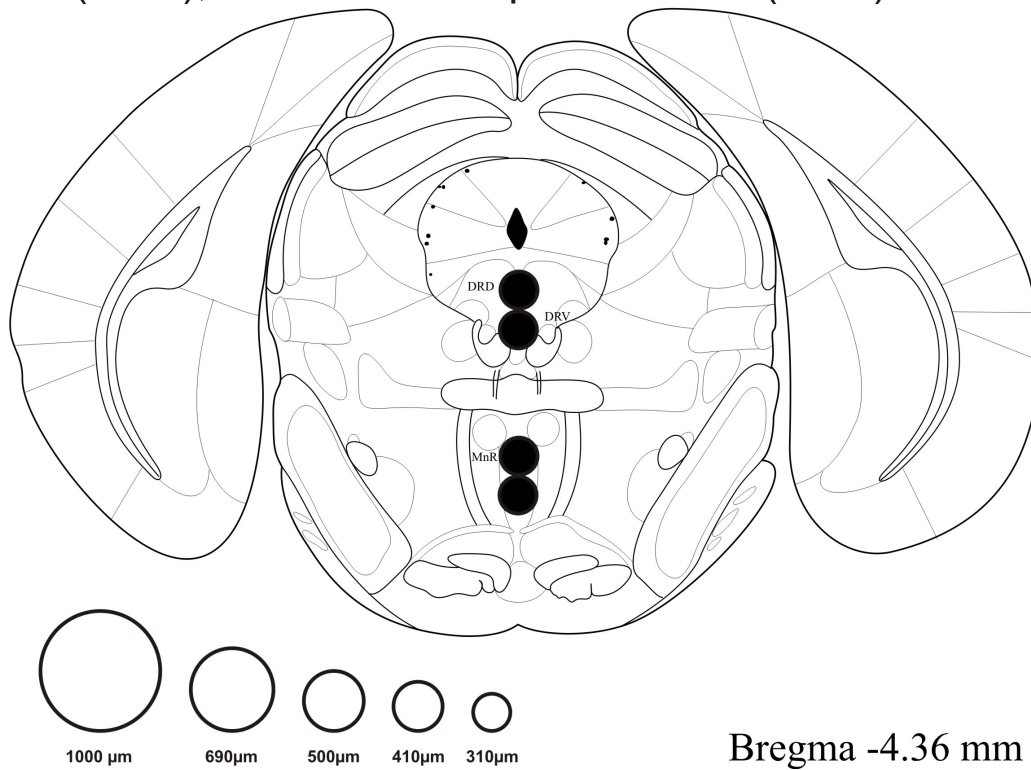
Cornu ammonis 1 of ventral hippocampus (CA1v)



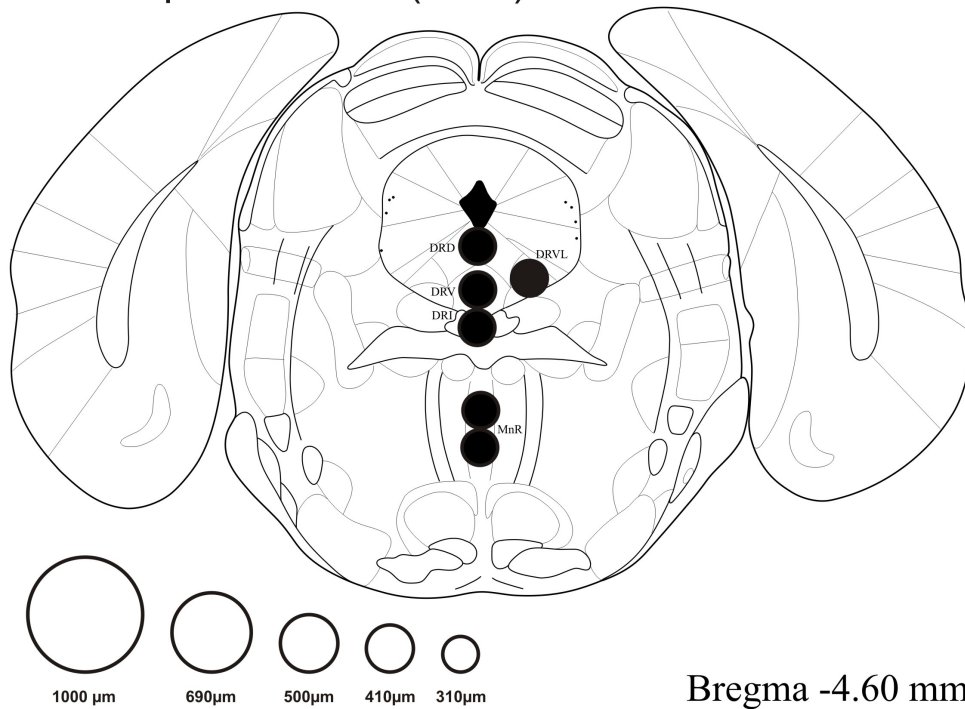
Cornu ammonis 1 of ventral hippocampus (CA1v)



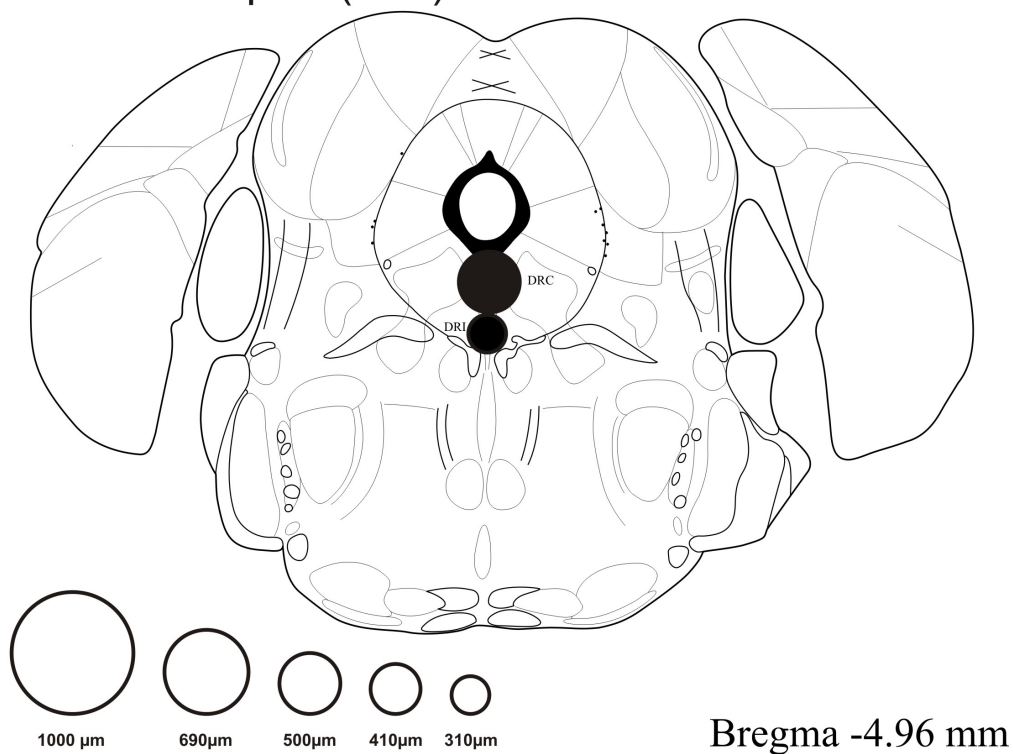
Dorsal raphe nucleus, dorsal part (DRD) and ventral part (DRV), and median raphe nucleus (MnR)



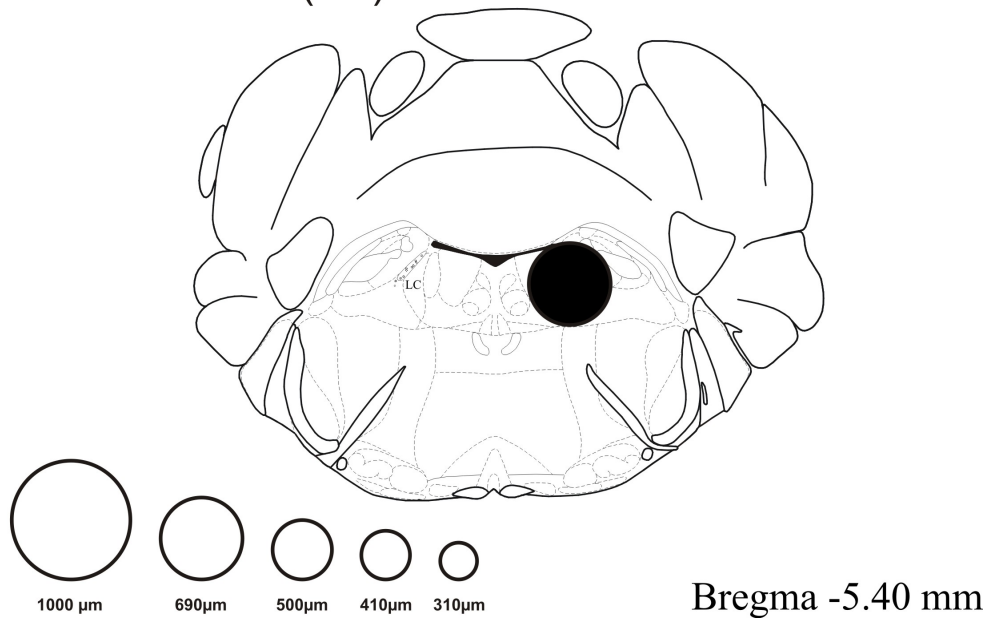
Dorsal raphe nucleus, dorsal part (DRD), ventral part (DRV), ventrolateral part/Ventrolateral periaqueductal gray (DRVL/VLPAG), and interfascicular part (DRI), and median raphe nucleus (MnR)



Dorsal raphe nucleus, caudal part (DRC) and interfascicular part (DRI)



Locus Coeruleus (LC)



Locus Coeruleus (LC)

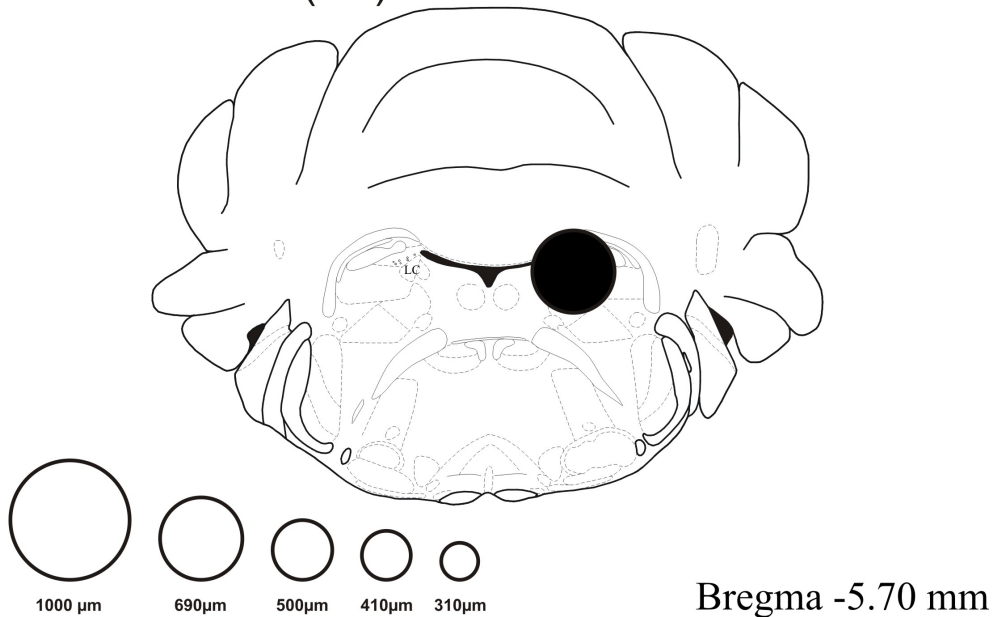


Fig. 2. Map of the microdissections in selected brain regions for both miR-19b OE and miR-19b KD experiments (abbreviations not indicated in plate titles: CPu = caudate putamen (striatum); LSD = lateral septal nucleus, dorsal part; LSV = lateral septal nucleus, ventral part; BSTMA = bed nucleus of the stria terminalis, medial division, anterior part; BSTMV = bed nucleus of the stria terminalis, medial division, ventral part; BSTLD = bed nucleus of the stria terminalis, lateral division, dorsal part; BSTLJ = bed nucleus of the stria terminalis, lateral division, juxtacapsular part; BSTLP = bed nucleus of the stria terminalis, lateral division, posterior part; BSTLV = bed nucleus of the stria terminalis, lateral division, ventral part; PaLM = paraventricular hypothalamic nucleus, lateral magnocellular part; PaDC = paraventricular hypothalamic nucleus, dorsal cap; PaMP = paraventricular hypothalamic nucleus, medial parvocellular part; PaMM = paraventricular hypothalamic nucleus, medial magnocellular part; PaV = paraventricular hypothalamic nucleus, ventral part; CA1 = field CA1 of the hippocampus) (Paxinos & Franklin, 2001).

calculate the concentration of the unknown samples. Tissue concentrations of NE and MHPG were standardized to the amount of protein in each microdissected structure.

2.7. Statistics

Student's *t*-test was used to assess significance in the absence of repeated measures. If neurochemical endpoints were compared across brain regions in the same subject, two-way analysis of variance (ANOVA) with repeated measures was used, with either miR-19b OE or KD as a between-subjects factor, and brain region as a within-subjects factor; post-hoc comparisons were made using Fisher's protected least significant difference (LSD) tests. Statistical analyses were performed using PASW (version 22.0, SPSS Inc., Chicago, IL) after elimination of statistical outliers (Grubbs, 1969). In order to run the repeated measures ANOVA, missing values were replaced using the Petersen method; these values were neither included in *post hoc* analyses, nor in any graphical representations of the data (Petersen, 1985).

3. Results

Reported results reflect data generated and analyzed at Dr. Christopher Lowry's Behavioral Neuroendocrinology Laboratory at the University of Colorado Boulder, Boulder, Colorado, from brain tissue harvested from animals that underwent the aforementioned experimental procedures; data generated from procedures conducted at Dr. Alon Chen's Neurobiology of Stress Laboratory in Rehovot, Israel, (i.e. behavioral testing) are considered to be beyond the scope of this thesis, and have thus been excluded from all following discussion.

3.1. miR-19b OE animals

Statistical analysis using two-factor repeated measures ANOVA revealed that there was a *treatment x region* interaction for the ratio of MHPG:NE ($F_{(4.56, 82.0)} = 3.38$; $p = 0.010$; $\epsilon = 0.285$). Region-specific *post hoc* testing for MHPG:NE ratios revealed BL miR-19b OE-induced decreases in the paraventricular nucleus of the hypothalamus (PVN; $p = 0.016$) and the dorsal hippocampus (CA1d; $p = 0.028$), as well as BL miR-19b OE-induced increases in the central nucleus of the amygdala (CeA; $p = 0.033$), the lateral septal nucleus, intermediate part (LSI; $p = 0.015$), and the dorsal raphe nucleus, ventral part (DRV; $p = 0.021$; Table 1; Fig. 3). A decrease in the ratio of MHPG:NE in the dorsal raphe nucleus, dorsal part (DRD) approached significance ($p = 0.052$).

Table 1. Average MHPG and NE concentrations, as well as MHPG:NE ratios in selected brain regions following either control conditions or miR-19b overexpression (miR-19b OE) 24 hours following completion of behavioral testing.

Brain Region	MHPG concentrations (pg/ μ g protein)		NE concentrations (pg/ μ g protein)		MHPG:NE	
	Control	miR-19b OE	Control	miR-19b OE	Control	miR-19b OE
PrL	2.56 \pm 0.10	2.73 \pm 0.11	9.70 \pm 0.39	9.31 \pm 0.15	0.27 \pm 0.015	0.29 \pm 0.011
IL	5.34 \pm 0.53	4.41 \pm 0.24	11.8 \pm 0.47	10.9 \pm 0.28	0.45 \pm 0.039	0.40 \pm 0.019
BnST	2.91 \pm 0.10	2.86 \pm 0.11	12.9 \pm 0.90	13.5 \pm 0.89	0.24 \pm 0.020	0.20 \pm 0.011
CeA	3.90 \pm 0.16	4.17 \pm 0.39	8.17 \pm 0.63	6.24 \pm 0.33	0.50 \pm 0.037	0.68 \pm 0.068*
BL	1.96 \pm 0.12	2.39 \pm 0.11*	8.57 \pm 0.37	9.11 \pm 0.43	0.23 \pm 0.016	0.25 \pm 0.011
PVN	3.80 \pm 0.37	3.09 \pm 0.17	46.6 \pm 6.52	57.9 \pm 5.13	0.093 \pm 0.011	0.058 \pm 0.007*
LSI	1.00 \pm 0.086	1.53 \pm 0.14**	8.44 \pm 0.36	9.21 \pm 0.36	0.12 \pm 0.008	0.17 \pm 0.016*
MS	2.61 \pm 0.18	2.65 \pm 0.23	9.75 \pm 0.58	8.39 \pm 0.57	0.29 \pm 0.027	0.29 \pm 0.007
CA1d	2.85 \pm 0.11	2.63 \pm 0.054	8.73 \pm 0.46	9.11 \pm 0.39	0.33 \pm 0.021	0.28 \pm 0.011*
CA1v	1.47 \pm 0.048	1.57 \pm 0.063	8.68 \pm 0.20	9.65 \pm 0.33	0.17 \pm 0.008	0.16 \pm 0.004
DRD	7.65 \pm 0.43	7.29 \pm 0.25	79.1 \pm 7.10	78.5 \pm 1.76	0.082 \pm 0.003	0.093 \pm 0.004
DRV	9.57 \pm 0.84	9.45 \pm 1.03	33.2 \pm 5.41	21.4 \pm 2.05	0.35 \pm 0.024	0.45 \pm 0.035*
DRI	9.47 \pm 0.55	8.59 \pm 0.49	16.1 \pm 0.79	14.6 \pm 1.05	0.59 \pm 0.019	0.64 \pm 0.037
DRVl	6.97 \pm 0.29	6.12 \pm 0.24*	26.2 \pm 3.55	24.3 \pm 2.27	0.27 \pm 0.033	0.27 \pm 0.027
DRC	11.5 \pm 1.31	11.5 \pm 1.64	20.5 \pm 2.10	25.2 \pm 3.57	0.53 \pm 0.058	0.47 \pm 0.039
MnR	2.64 \pm 0.12	2.62 \pm 0.082	8.32 \pm 0.40	8.30 \pm 0.11	0.32 \pm 0.023	0.33 \pm 0.008
LC	6.25 \pm 0.58	7.82 \pm 0.68	40.5 \pm 7.81	48.9 \pm 6.64	0.15 \pm 0.016	0.16 \pm 0.011

(abbreviations: PrL = prelimbic cortex; IL = infralimbic cortex; BnST = bed nucleus of the stria terminalis; CeA = central nucleus of the amygdala; BL = basolateral amygdaloid nucleus; PVN = paraventricular nucleus of the hypothalamus; LSI = lateral septal nucleus, intermediate part; MS = medial septal nucleus; CA1d = field cornu ammonis 1 of the hippocampus, dorsal region; CA1v = field cornu ammonis 1 of the hippocampus, ventral region; DRD = dorsal raphe nucleus, dorsal part; DRV = dorsal raphe nucleus, ventral part; DRI = dorsal raphe nucleus, interfascicular part; DRVl = dorsal raphe nucleus, ventrolateral part; DRC = dorsal raphe nucleus, caudal part; MnR = median raphe nucleus; LC = locus coeruleus) (Paxinos & Franklin, 2001). Values are presented as mean \pm S.E.M. * $p < 0.05$, ** $p < 0.01$, *** $p < 0.001$, compared with mice injected with control lentivirus (Fisher's protected least significant difference tests).

Statistical analyses using two-factor repeated measures ANOVA for MHPG concentrations revealed no significant main effect of *treatment* ($F_{(1,00, 18.0)} = 0.13$; $p = 0.728$; $\epsilon = 0.174$) or *treatment* \times *region* ($F_{(2,78, 50.1)} = 0.76$; $p = 0.514$; $\epsilon = 0.174$) interaction.

Region-specific *post hoc* testing was conducted for MHPG concentrations and the ratios of MHPG:NE regardless of whether observed main or interaction effects were present on the justification that *a priori* reasoning presents a theoretical basis in which we would expect to see changes in NE metabolism in specific brain regions as a result of alterations in NE transmission in the BL. We believe these changes may remain undetected by ANOVA testing due to the large

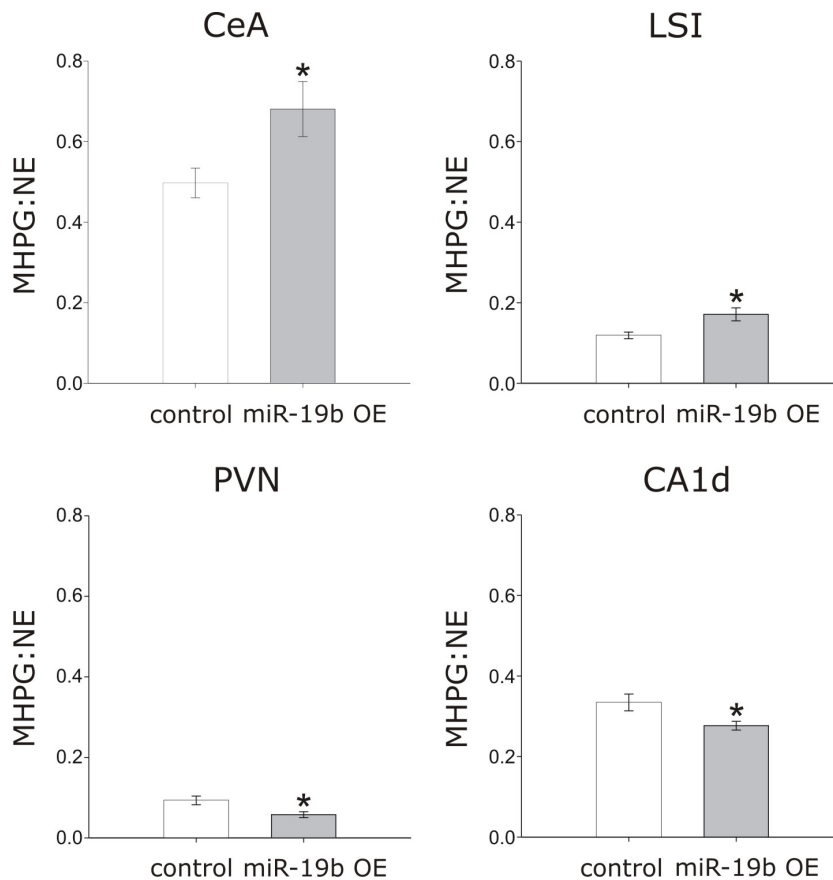


Fig. 3. Graphs illustrating the effects of injections of either control or miR-19b OE viral vectors on noradrenergic metabolism. Graphs illustrate the ratio of MHPG:NE concentrations in selected brain regions. * $p < 0.05$ compared with mice injected with control lentivirus (Fisher's protected least significant difference tests). Bar graphs represent the means \pm S.E.M. (CeA: $n = 10$ for control, $n = 10$ for miR-19 OE; PVN: $n = 10$ for control, $n = 8$ for miR-19 OE; LSI: $n = 10$ for control, $n = 8$ for miR-19 OE; CA1d: $n = 10$ for control, $n = 8$ for miR-19 OE). For abbreviations, see Figure 2.

number of brain regions examined. As many of these regions may not have expressed significant changes in NE metabolism due to experimental manipulation, these null results have the potential of masking the presence of relatively small effect sizes to ANOVA detection. Furthermore, as MHPG concentrations and MHPG:NE ratios are both viable measures of NE metabolism, the most thorough investigation into changes in NE metabolism as a result of experimental manipulation must include a comparison of similarities and differences across both measures; thus, we justify that specific comparisons by brain-region may be made for MHPG concentrations and MHPG:NE ratios regardless of the outcome of the corresponding overall F test (Winer et al., 1991).

Region-specific *post hoc* testing for MHPG concentrations revealed a BL miR-19b OE-induced decrease in the dorsal raphe nucleus, ventrolateral part (DRVl; $p = 0.037$), as well as BL miR-19b OE-induced increases in the BL ($p = 0.018$) and the LSI ($p = 0.006$). A decrease in

MHPG concentrations in the CA1d approached significance ($p = 0.100$), as did an increase in MHPG concentrations in the LC ($p = 0.097$).

Statistical analyses using two-factor repeated measures ANOVA for NE concentrations revealed no significant main effect of *treatment* ($F_{(1.00, 18.0)} = 0.05$; $p = 0.822$; $\epsilon = 0.224$) or *treatment x region* ($F_{(3.58, 64.5)} = 1.42$; $p = 0.241$; $\epsilon = 0.224$) interaction.

3.2. *miR-19b* KD animals

Statistical analysis using two-factor repeated measures ANOVA revealed no significant *treatment x region* ($F_{(3.32, 73.0)} = 1.60$; $p = 0.194$; $\epsilon = 0.207$) interaction for the ratio of MHPG:NE; however, a main effect of treatment approached significance ($F_{(1.00, 22.0)} = 3.29$; $p = 0.083$; $\epsilon = 0.207$).

For justification of *post hoc* testing in the absence of observed *treatment* or *treatment x region* interactions, see section 3.1.

Region-specific *post hoc* testing for MHPG:NE ratios revealed a BL *miR-19b* KD-induced decrease in the LSI ($p = 0.023$), as well as BL *miR-19b* KD-induced increases in the PVN ($p = 0.003$), the CA1d ($p = 0.020$), the BnST ($p = 0.001$), and the CA1v ($p < 0.001$) (Table 2; Fig. 4). The decrease in the ratio of MHPG:NE in the dorsal raphe nucleus, interfascicular part (DRI) approached significance ($p = 0.053$).

Table 2 . Average MHPG and NE concentrations, as well as MHPG:NE ratios in selected brain regions following either control conditions or miR-19b knockdown (miR-19b KD) 24 hours following completion of behavioral testing.

Brain Region	MHPG concentrations (pg/ μ g protein)		NE concentrations (pg/ μ g protein)		MHPG:NE	
	Control	miR-19b KD	Control	miR-19b KD	Control	miR-19b KD
PrL	1.20 \pm 0.060	1.16 \pm 0.10	4.45 \pm 0.31	4.37 \pm 0.23	0.26 \pm 0.012	0.27 \pm 0.023
IL	1.33 \pm 0.14	1.80 \pm 0.26	6.81 \pm 0.33	6.70 \pm 0.39	0.21 \pm 0.036	0.21 \pm 0.012
BnST	1.22 \pm 0.085	1.57 \pm 0.10*	9.14 \pm 0.28	6.73 \pm 0.65	0.13 \pm 0.010	0.26 \pm 0.025**
CeA	1.10 \pm 0.16	1.01 \pm 0.087	3.21 \pm 0.18	2.94 \pm 0.17	0.32 \pm 0.043	0.35 \pm 0.031
BL	1.07 \pm 0.046	1.17 \pm 0.059	3.95 \pm 0.30	4.36 \pm 0.15	0.25 \pm 0.016	0.27 \pm 0.013
PVN	2.10 \pm 0.12	2.89 \pm 0.14***	22.0 \pm 2.21	18.4 \pm 2.12	0.096 \pm 0.009	0.16 \pm 0.016**
LSI	0.86 \pm 0.058	0.81 \pm 0.083	3.80 \pm 0.31	3.87 \pm 0.34	0.23 \pm 0.015	0.18 \pm 0.012*
MS	4.21 \pm 0.30	5.59 \pm 0.38*	8.15 \pm 0.67	8.32 \pm 0.28	0.56 \pm 0.074	0.68 \pm 0.078
CA1d	1.13 \pm 0.071	1.38 \pm 0.11	6.28 \pm 0.20	6.66 \pm 0.20	0.17 \pm 0.006	0.21 \pm 0.014*
CA1v	1.24 \pm 0.054	1.40 \pm 0.074	5.64 \pm 0.28	4.36 \pm 0.15	0.23 \pm 0.015	0.33 \pm 0.017***
DRD	2.13 \pm 0.080	2.19 \pm 0.16	34.6 \pm 1.53	40.0 \pm 1.64	0.063 \pm 0.003	0.056 \pm 0.004
DRV	2.06 \pm 0.065	2.39 \pm 0.18	11.7 \pm 0.68	13.6 \pm 0.81	0.18 \pm 0.011	0.18 \pm 0.016
DRI	1.70 \pm 0.086	1.60 \pm 0.089	5.55 \pm 0.18	6.27 \pm 0.081	0.31 \pm 0.021	0.26 \pm 0.015
DRVl	2.20 \pm 0.10	2.39 \pm 0.12	14.0 \pm 1.77	15.2 \pm 2.35	0.18 \pm 0.027	0.20 \pm 0.030
DRC	2.00 \pm 0.15	2.97 \pm 0.43*	7.21 \pm 0.82	10.2 \pm 1.36	0.29 \pm 0.021	0.27 \pm 0.015
MnR	3.51 \pm 0.10	3.93 \pm 0.21	5.24 \pm 0.16	6.28 \pm 0.33	0.67 \pm 0.015	0.63 \pm 0.031
LC	7.44 \pm 0.91	9.09 \pm 1.25	23.4 \pm 5.69	28.7 \pm 6.73	0.41 \pm 0.072	0.53 \pm 0.095

(abbreviations: PrL = prelimbic cortex; IL = infralimbic cortex; BnST = bed nucleus of the stria terminalis; CeA = central nucleus of the amygdala; BL = basolateral amygdaloid nucleus; PVN = paraventricular nucleus of the hypothalamus; LSI = lateral septal nucleus, intermediate part; MS = medial septal nucleus; CA1d = field cornu ammonis 1 of the hippocampus, dorsal region; CA1v = field cornu ammonis 1 of the hippocampus, ventral region; DRD = dorsal raphe nucleus, dorsal part; DRV = dorsal raphe nucleus, ventral part; DRI = dorsal raphe nucleus, interfascicular part; DRVl = dorsal raphe nucleus, ventrolateral part; DRC = dorsal raphe nucleus, caudal part; MnR = median raphe nucleus; LC = locus coeruleus) (Paxinos & Franklin, 2001). Values are presented as mean \pm S.E.M. * $p < 0.05$, ** $p < 0.01$, *** $p < 0.001$, compared with mice injected with control lentivirus (Fisher's protected least significant difference tests).

Statistical analysis using two-factor repeated measures ANOVA revealed no significant *treatment x region* ($F_{(1.63, 35.9)} = 1.42$; $p = 0.253$; $\epsilon = 0.102$) interaction for MHPG concentrations; however, a main effect of *treatment* was observed ($F_{(1.00, 22.0)} = 8.00$; $p = 0.010$; $\epsilon = 0.102$). Region-specific *post hoc* testing for MHPG concentrations revealed BL miR-19b KD-induced increases in the bed nucleus of the stria terminalis (BnST; $p = 0.017$), the PVN ($p < 0.001$), the medial septal nucleus (MS; $p = 0.010$), and the dorsal raphe nucleus, caudal part (DRC; $p = 0.049$). The increases in MHPG concentrations in the CA1d ($p = 0.077$), the ventral

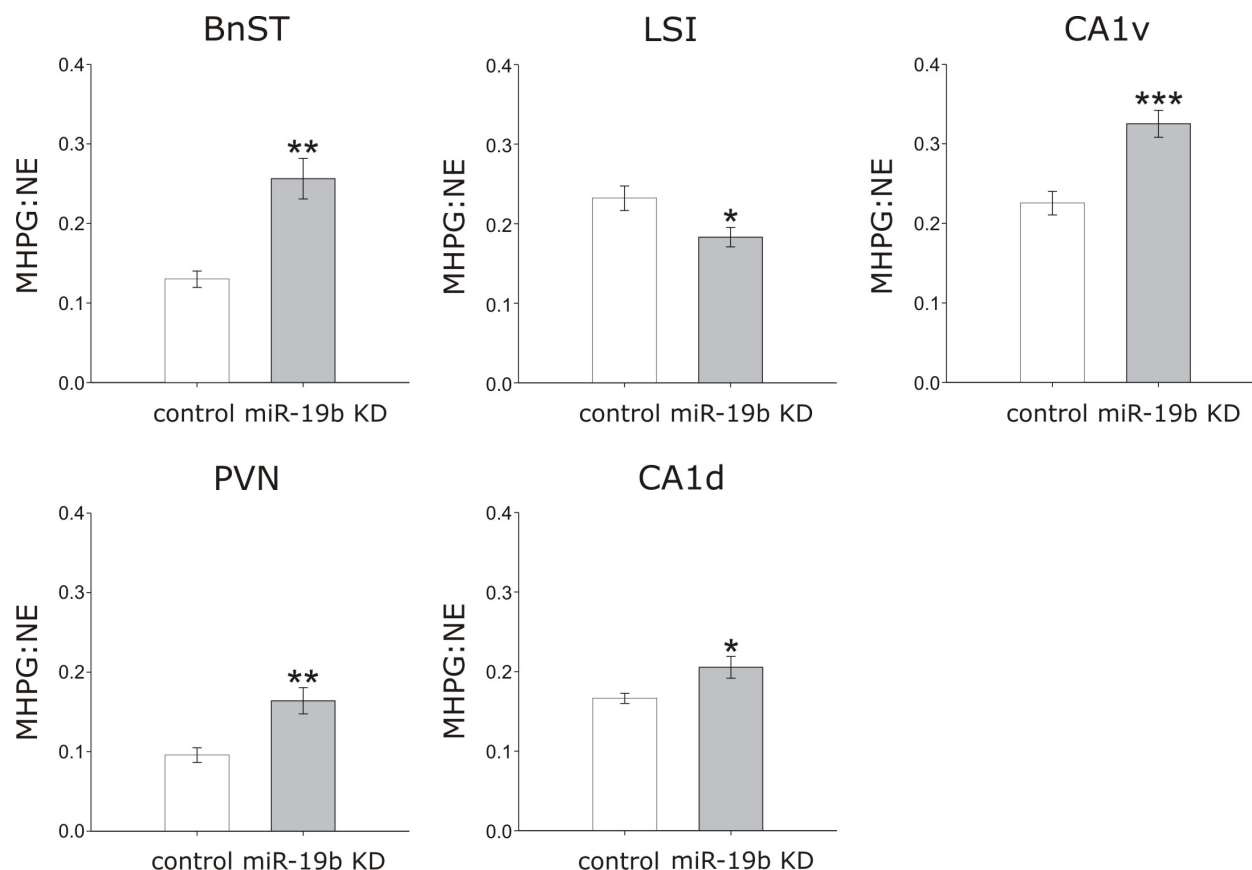


Fig. 4. Graphs illustrating the effects injections of either control or miR-19b KD viral vectors on noradrenergic metabolism. Graphs illustrate the ratio of MHPG:NE concentrations in selected brain regions. * $p < 0.05$; ** $p < 0.01$; *** $p < 0.001$ compared with mice injected with control lentivirus (Fisher's protected least significant difference tests). Bar graphs represent the means \pm S.E.M. (BnST: $n = 10$ for control, $n = 10$ for miR-19b KD; PVN: $n = 11$ for control, $n = 9$ for miR-19b KD; LSI: $n = 11$ for control, $n = 10$ for miR-19b KD; CA1d: $n = 10$ for control, $n = 12$ for miR-19b KD; CA1v: $n = 12$ for control, $n = 11$ for miR-19b KD). For abbreviations, see Figure 2.

hippocampus (CA1v; $p = 0.092$), and the median raphe nucleus (MnR; $p = 0.083$) approached significance.

Statistical analyses using two-factor repeated measures ANOVA for NE concentrations revealed no significant main effect of *treatment* ($F_{(1.00, 22.0)} = 0.52$; $p = 0.477$; $\epsilon = 0.104$) or *treatment x region* ($F_{(1.67, 36.7)} = 0.94$; $p = 0.385$; $\epsilon = 0.104$) interaction.

4. Discussion

Our data support an effect of miR-19b, acting within the BL, on noradrenergic signaling in brain areas downstream of the BL. As unpublished data from the Chen laboratory conclude that miR-19b targets the *Adrb1* to downregulate its expression, we can conclude that modulation of miR-19b transcription in the BL also ultimately affects noradrenergic transmission in downstream targets. Furthermore, more unpublished data from the Chen laboratory indicate

that modulation of miR-19b in the BL affects stress-associated behavioral outputs, suggesting that miR-19b associated with the Ago2 complex plays a key role in the mediation of the stress response, likely through the aforementioned altered noradrenergic transmission seen in downstream targets. Reciprocal changes in NE metabolism, as quantified by both MHPG concentrations and the ratio of MHPG:NE, were observed in the PVN, the CA1d, and the LSI. While experimental manipulations yielded strong effects in the BnST for miR-19b KD, no changes were observed for miR-19b OE in this brain region. Finally, changes in NE metabolism in the DRVL, the BL, the CeA, and the DRV for miR-19b OE, and the MS and DRC for miR-19b KD were observed that were isolated to only one measurement of NE metabolism per given experiment, and complementary changes were not observed in the other respective experiment.

An effect of altered noradrenergic transmission in the BL was observed in the hippocampus for both miR-19b KD and miR-19b OE. An increase in the ratio of MHPG:NE in the CA1d for miR-19b KD was accompanied by a reciprocal decrease for miR-19b OE. Glutamatergic projection neurons within the BL, which project directly to a number of limbic forebrain structures, including the prefrontal cortex (McDonald, 1991) and the hippocampus (Pikkarainen et al., 1999), are known to respond in an excitatory fashion to the stimulation of β -adrenergic receptors (Buffalari and Grace, 2007), and these neurons are thought to release glutamate presynaptically to enhance NE release in these projection targets (Russell and Wiggins, 2000; Howells and Russell, 2008; Dazzi et al., 2011). Therefore, we predicted that the OE and KD experiments respectively would yield reciprocal changes in NE metabolism in specific downstream BL projection targets. As selective upregulation (OE) or knockdown (KD) of miR-19b transcription induces reciprocal changes in *Adrb1* levels, we predicted a negative correlation between miR-19b levels and the activation of the glutamatergic networks that act to induce presynaptic modulation of NE transmission in downstream BL projection targets. Consequently, these findings are consistent with our predictions. Furthermore, as noradrenergic innervation of the BL mainly originates from the LC (Asan, 1998), a hypothetical neural circuit can be proposed in which changes in *Adrb1* density in the BL alter noradrenergic input primarily from the LC onto efferent glutamatergic neurons projecting to downstream BL target structures (Fig. 5).

While significant effects of both miR-19b OE and KD on MHPG:NE ratios in the CA1d were observed, complementary effects in MHPG concentrations were not observed in either of the experiments; however, the decrease in the ratio of MHPG:NE in the CA1d observed for miR-19b OE was accompanied by a decrease in MHPG concentrations in the CA1d that approached significance, and the increases in the ratio of MHPG:NE in the CA1d and the CA1v observed

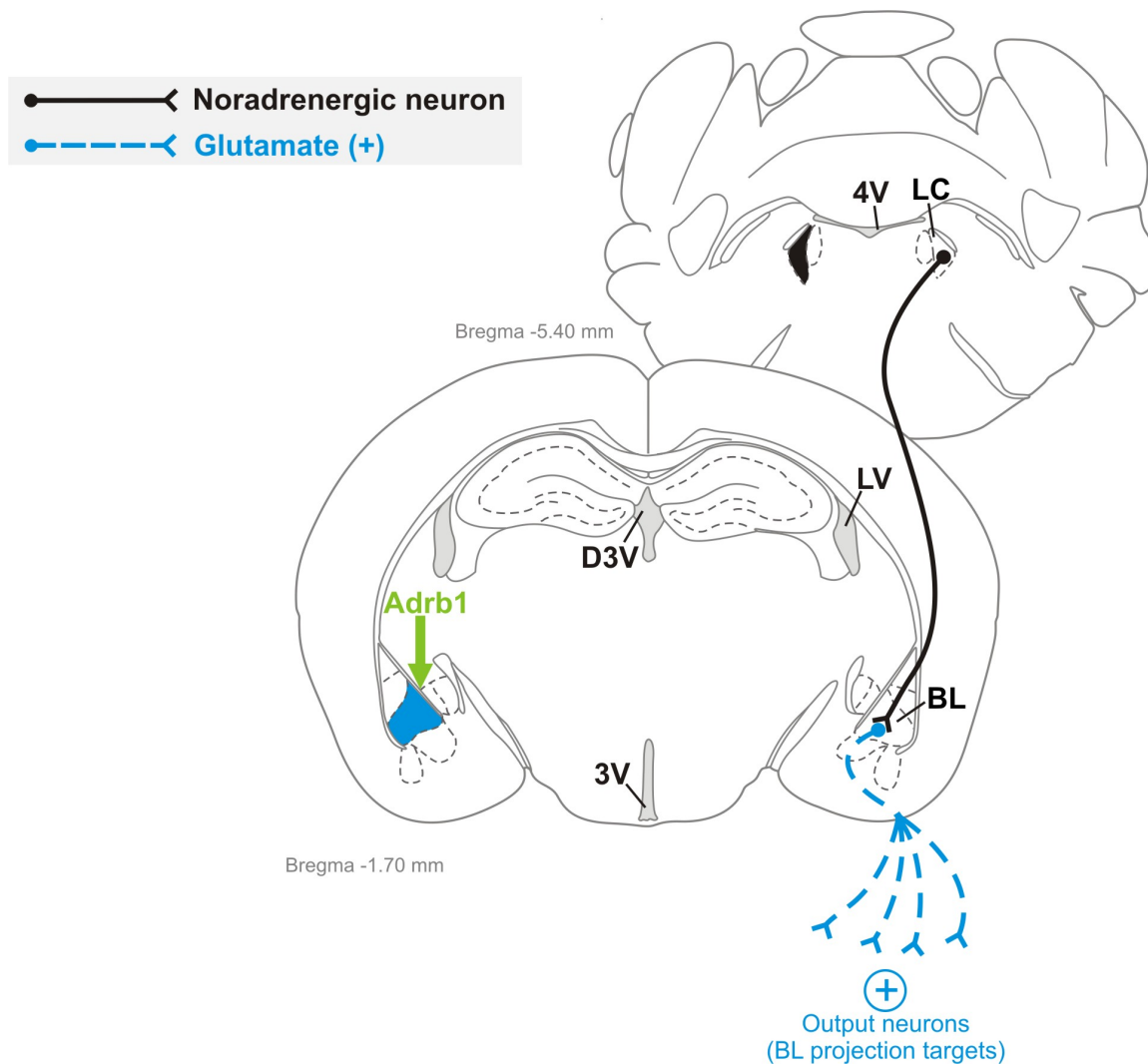


Fig. 5. Hypothetical neural circuit model demonstrating the effects of modulating noradrenergic transmission in the basolateral amygdala (BL) on activity of BL glutamatergic projection neurons. For abbreviations, see Figure 2. (abbreviations not previously listed: LV = lateral ventricle; 3V = third ventricle; D3V = dorsal third ventricle; 4V = fourth ventricle) (Paxinos & Franklin, 2001).

for miR-19b KD were accompanied by increases in both the CA1d and CA1v that also approached significance. Given that the BL is known to project to the hippocampus to mediate the consolidation of explicit/associative memories through the activation of β -adrenoreceptors, purportedly by a glucocorticoid-sensitive mechanism (Pikkarainen et al., 1999; Roozendaal 2000), we expected to see changes in NE metabolism in hippocampal nuclei as a result of altered ADRB1 density in the BL. Thus, there is compelling evidence to support the notion that the aforementioned changes in MHPG concentrations in hippocampal nuclei that merely approached significance were indeed real effects that failed to reach significance as a result of type II statistical error, or the study was insufficiently powered to detect the effects.

Reciprocal changes between both miR-19b OE and KD protocols were also observed in the PVN for MHPG:NE ratios, in addition to complementary changes in both MHPG concentrations and the ratio of MHPG:NE for miR-19b KD. A decrease in MHPG concentrations was observed for miR-19b OE, while increases in MHPG concentrations and the ratio of MHPG:NE were observed for miR-19b KD; however, though noradrenergic signaling is thought to play an important regulatory role in the neurosecretory secretions of the PVN of both parvocellular and magnocellular neurons (Daftary et al., 2000; Daftary et al., 1998), the changes in NE metabolism observed in this brain region as a result of alterations in *Adrb1* density are likely not direct, as the BL is thought to only project indirectly to this brain region (Ulrich-Lai and Herman, 2009). Nonetheless, NE has been shown to stimulate corticotropin-releasing hormone (CRH) gene expression in the parvocellular division of the PVN and consequent CRH release into the portal circulation of the median eminence (Itoi et al., 1994), thereby suggesting a role for miR-19b acting in the BL to affect the hypothalamic-pituitary-adrenal (HPA) axis response to stress by influencing CRH and adrenocorticotrophic hormone (ACTH) secretion as a result of altered NE signaling in the PVN.

A somewhat perplexing decrease in the LSI in the ratio of MHPG:NE for miR-19b KD was accompanied by reciprocal increases for miR-19b OE in both the ratio of MHPG:NE and MHPG concentration data. These changes are in opposition to the changes observed in previously mentioned forebrain structures (i.e. the PVN and the CA1d), as all other previously mentioned changes in NE metabolism for miR-19 OE were decreases, while all other previously mentioned changes in NE metabolism for miR-19b KD were increases. Changes in the LSI were expected, as the BL is known to send projections to the lateral septum (Kita and Kitai, 1990); however, the opposing effects of glutamatergic efferent projections leaving the BL are likely to be mediated indirectly (multisynaptically) through intrinsic GABAergic networks that act to exert local control on noradrenergic transmission (Paré & Duvarci, 2012). Based on this information, a hypothetical neural circuit can be proposed in which glutamatergic neurons projecting from the BL to downstream targets act both directly and indirectly via intrinsic GABAergic networks to presynaptically modulate noradrenergic transmission in projection targets (Fig. 6). The LSI has long been known to share extensive efferent connections with the hypothalamus (Swanson & Cowan 1979; Garris 1979), and has been implicated as a relay station for communication between the somatic and autonomic nervous systems in the coordination of the limbic response (Staiger & Nürnberg, 1991). These pathways may provide further downstream circuitry by which miR-19b acting in the BL might modulate the HPA response to stress.

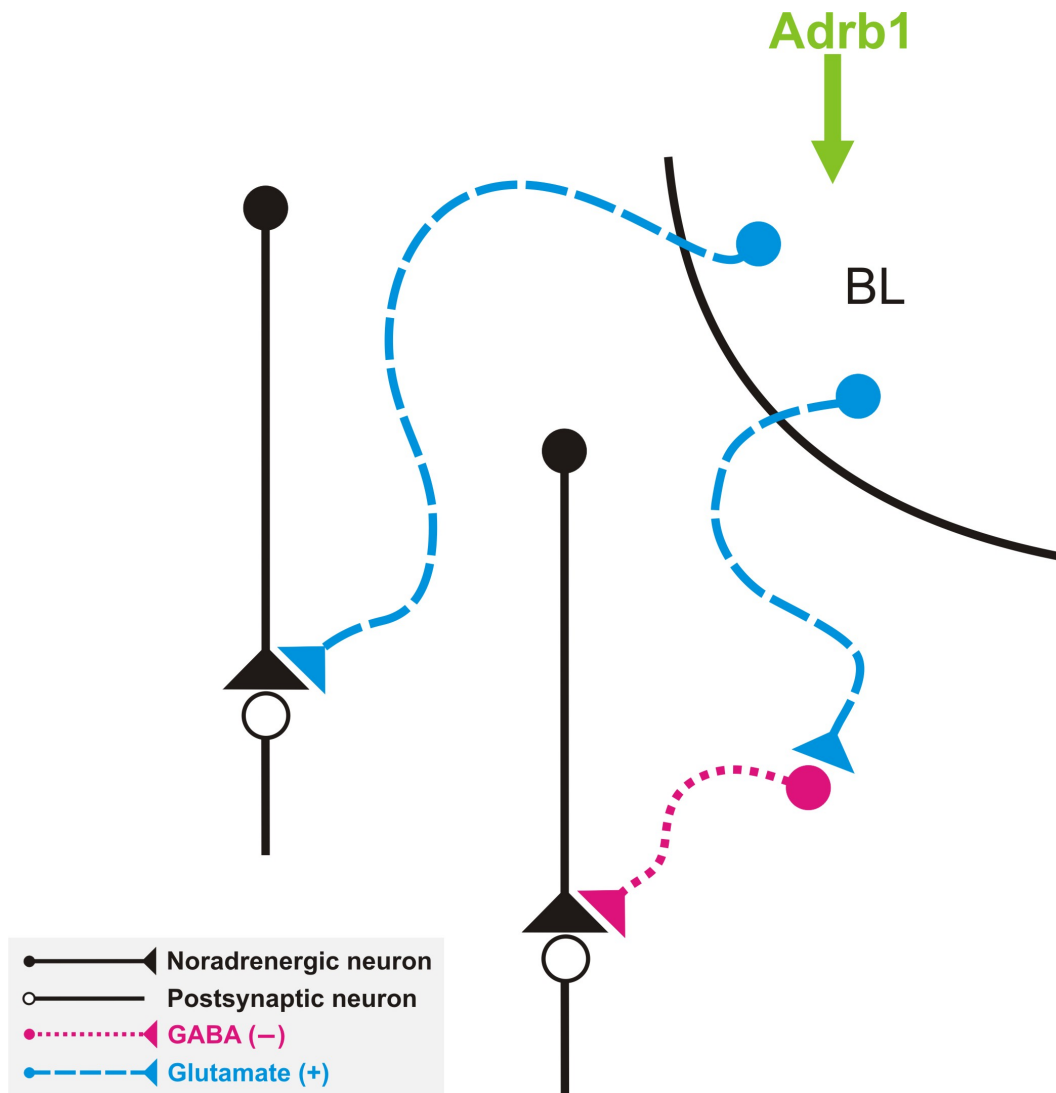


Fig. 6. Hypothetical neural circuit model depicting the methods by which glutamatergic outputs from the basolateral amygdala (BL) may modulate noradrenergic transmission in noradrenergic terminals without altering noradrenergic activity in the locus coeruleus (LC).

The BnST yielded strong effects for miR-19b KD, showing increases in both MHPG concentrations and the ratio of MHPG:NE. Though they are somewhat more limited in number than other amygdalar projections to the same region, the BL is known to send projections directly to the BnST (Dong et al., 2001b); thus, changes in NE metabolism in the BnST as a result of experimental manipulation were expected. That changes were observed in both ratio and MHPG data for miR-19b KD reinforces the validity of these respective observations. That no changes in NE metabolism – as determined by either measure – were observed for miR-19b OE is likely due to type II statistical error in which we failed to detect the presence of an effect due to *Adrb1* downregulation in the BL. As discussed later, decreases in NE transmission are

likely to be much harder to detect than increases in NE transmission, and this fact, coupled with the presence of strong effects in both measures as observed in the KD experiment provide strong evidence in support of the presence of type II error in the *post hoc* analysis of BnST effects in the OE experiment. The BnST is known to project to the PVN in order to regulate HPA axis responses to stress, with the anteroventral subregions of the BnST implicated in acute activation of PVN neurons, and the posteromedial subregions of the BnST implicated in the inhibition of HPA activity in response to stress, likely by acting on GABAergic neurons in the PVN (Choi et al., 2007; Gray et al., 1993; Cullinan et al., 2004). Furthermore, the anterolateral BnST is known to project to the PVN via CRH neurons (Dong et al., 2001a; Champagne et al., 1998), which suggests a mechanism for central control of the HPA axis via excitatory actions of CRH produced in the BnST (Ulrich-Lai and Herman, 2009). These data further support the conclusion that miR-19b acting in the BL can affect key structures responsible for mediating the HPA axis response to stress.

Changes in MHPG concentrations were observed in the DRVL and the BL for miR-19b OE. Additionally, changes in MHPG:NE ratios were observed in the CeA and the DRV for miR-19b OE. No changes in NE metabolism were observed for miR-19 KD for any of these brain structures by either measure of NE metabolism (MHPG concentrations and the ratio of MHPG:NE respectively). Of these structures, there was evidence to support the prediction of a change in NE metabolism in the CeA as a direct result of alteration in signaling from the BL given that it has been demonstrated that the CeA is an intra-amygdaloid target of projections arising from the basolateral nuclei, which serve as a relay between the lateral nucleus and the CeA in the communication of auditory fear conditioning of the Pavlovian type (Paré et al., 1995). The increase that was observed in the MHPG:NE ratio as measured in the CeA supports the model proposed by Paré and Duvarci (2012), in which local GABAergic circuitry is thought to play a role in the relay of intra-amygdaloid signals. A prediction of the change in MHPG concentration in the BL that was observed was not theoretically supported by existing literature, though this observation could have been precipitated by intra-BL projections that acted to modulate NE release within the BL. Any changes observed in dorsal raphe nucleus (DRN) structures were theorized to be mediated by indirect downstream pathways prior to experimentation (Ulrich-Lai and Herman, 2009), and thus were not to be considered direct (monosynaptic) results of experimental manipulation. Due to the polysynaptic nature of changes observed in DRN structures as a result of altered NE signaling in the BL, it is difficult to theorize on the exact nature of these connections and their physiological implications without further study.

Changes in MHPG concentrations were observed in the MS and the DRC for miR-19b KD. No changes in NE metabolism were observed in the OE experiment for either of these brain structures by either measure of NE metabolism (MHPG concentrations and the ratio of MHPG:NE respectively). The MS is thought to act in a similar fashion to the LSI by serving as a relay for coordination of autonomic and somatic responses between prominent limbic areas (Staiger and Nürnberger, 1991). Though the MS is known to have extensive projections to hypophysiotropic nuclei (Garris 1979), the physiological significance of this change is unclear, as projections from the BL to the MS have not previously been reported (Krettek and Price, 1978). Further studies would need to be conducted in order to more accurately postulate on circuitry mediating BL influences on noradrenergic metabolism in the DRC.

As we are considering both MHPG concentrations and the ratio of MHPG:NE to be viable measures of NE metabolism, we can infer that the data set is more reliable when we observe a greater correlation in specific brain structures between changes observed in NE metabolism as measured by MHPG concentrations and changes observed in NE metabolism as measured by the ratio of MHPG:NE within the same experiment. Greater correlations between the two measures were observed for miR-19b KD, where complementary changes in both MHPG concentrations and the ratio of MHPG:NE were observed in the PVN, CA1d, CA1v, and BnST, as opposed to miR-19b OE, in which complementary changes were observed only in the CA1d and the LSI across both measures (note that MHPG concentrations in the hippocampal regions only approached significance). This is likely because it is easier to detect changes in NE metabolism resulting from an increase in noradrenergic signaling in the BL, as was the experimental manipulation performed via miR-19b KD, rather than changes in NE metabolism resulting from decreases in noradrenergic signaling in the BL, as was the experimental manipulation performed via miR-19b OE.

In conclusion, our data have shown that modulation of BL-specific miR-19b expression can effectively influence distributed systems in the brain responsible for the regulation of key components of anxiety and fear paradigms in animal models, such as emotional stress (Tanaka et al., 2000) and memory consolidation (Roosendaal, 2000), both of which are believed to share inherently similar neural circuitry with human anxiety disorders (Bouton et al., 2001; Pitman et al., 1999; Sullivan et al., 2003). However, it is important to note that miR-19b is known to target mRNA's other than those associated with the *Adrb1* (e.g. Zhang et al., 2011; Lakner et al., 2012), and thus there exists the possibility that some of the observed effects of miR-19b acting in the BL were not *Adrb1* dependent, but rather the result of altered expression of other proteins. Despite these limitations, our data still support the hypothesis that manipulation of BL-

specific *Adrb1* expression may provide a deeper understanding of anxiety and affective disorders, which may one day lead to more effective therapeutics that will serve to improve the overall human condition and positively affect quality of life factors for afflicted individuals.

4.1. Future directions

The current study can serve to guide future studies on NE signaling in brain regions of interest downstream of altered NE transmission in the BL. It would be of particular interest to examine NE release via microdialysis in target brain regions to observe changes over time as a result of experimental manipulation. Furthermore, as we hypothesize that the BL exerts its influence on NE signaling in downstream structures via glutamatergic outputs, it would be interesting to see if we could effectively block the effects of miR-19b OE or KD treatment by administering a glutamate antagonist in select brain regions to verify our current understanding of this particular neural circuitry.

References

- Asan, E (1998) The catecholaminergic innervation of the rat amygdala. *Adv Anat Embryol Biol* 142:1-118.
- Bouton ME, Mineka S, Barlow DH (2001) A modern learning theory perspective on the etiology of panic disorder. *Psychol Rev* 108(1):4-32.
- Buffalari DM, Grace AA (2007) Noradrenergic modulation of basolateral amygdala neuronal activity: opposing influences of α -2 and β receptor activation. *J Neurosci* 27(45):12358-12366.
- Champagne D, Beaulieu J, Drolet G (1998) CRFergic innervation of the paraventricular nucleus of the rat hypothalamus: a tract-tracing study. *J Neuroendocrinol* 10:119-131.
- Chen F-J, Sara SJ (2007) Locus coeruleus activation by foot shock or electrical stimulation inhibits amygdala neurons. *Neuroscience* 144:472-481.
- Choi DC, Furay AR, Evanson NK, Ostrander MM, Ulrich-Lai YM, Herman JP (2007) Bed nucleus of the stria terminalis subregions differentially regulate hypothalamic-pituitary-adrenal axis activity: implications for the integration of limbic inputs. *J Neurosci* 27(8):2025-2034.
- Cullinan WE, Herman JP, Watson SJ (2004) Ventral subicular interaction with the hypothalamic paraventricular nucleus: evidence for a relay in the bed nucleus of the stria terminalis. *J Comp Neurol* 332(1):1-20.
- Daftary SS, Boudaba C, Szabó K, Tasker JG (1998) Noradrenergic excitation of magnocellular neurons in the rat hypothalamic paraventricular nucleus via intranuclear glutamatergic circuits. *J Neurosci* 18(24):10619-10628.
- Daftary SS, Boudaba C, Tasker JG (2000) Noradrenergic regulation of parvocellular neurons in the rat hypothalamic paraventricular nucleus. *Neuroscience* 96(1):743-751.
- Dahlström A, Fuxe K (1964) Evidence for the existence of monoamine-containing neurons in the central nervous system. *Acta Physiol Scand* 62:5-52.
- Damasio AR (1998) Emotion in the perspective of an integrated nervous system. *Brain Res Brain Res Rev* 26:83-86.
- Dazzi L, Matzeu A, Biggio G (2011) Role of ionotropic glutamate receptors in the regulation of hippocampal norepinephrine output in vivo. *Brain Res* 1386:41-49.
- Dong H-W, Petrovich GD, Watts AG, Swanson LW (2001a) Basic organization of projections from the oval and fusiform nuclei of the bed nuclei of the stria terminalis in adult rat brain. *J Comp Neurol* 436:430-455.
- Dong H-W, Petrovich GD, Swanson LW (2001b) Topography of projections from amygdala to bed nuclei of the stria terminalis. *Brain Res Brain Res Rev* 38:192-246.
- Evans AK, Reinders N, Ashford KA, Christie IN, Wakerley JB, Lowry CA (2008) Evidence for serotonin synthesis-dependent regulation of in vitro neuronal firing rates in the midbrain raphe complex. *Eur J Pharmacol* 590:136-149.
- Fallon JH, Koziell DA, Moore RY (1978) Catecholamine innervation of the basal forebrain. II. Amygdala, suprarhinal cortex and entorhinal cortex. *J Comp Neurol* 180(3):509-532.
- Ferry B, Magistretti PJ, Pralong E (1997) Noradrenaline modulates glutamate-mediated neurotransmission in the rat basolateral amygdala in vitro. *Eur J Neurosci* 9:1356-1364.
- Fu A, Li X, Zhao B (2008) Role of β ₁-adrenoceptor in the basolateral amygdala of rats with anxiety-like behavior. *Brain Res* 1211:85-92.
- Garris DR (1979) Direct septo-hypothalamic projections in the rat. *Neurosci Lett* 13:82-90.
- Gean PW, Huang CC, Lin JH, Tsai JJ (1992) Sustained enhancement of NMDA receptor-mediated synaptic potential by isoproterenol in rat amygdala slices. *Brain Res* 594:331-334.
- Gray TS, Piechowski RA, Yracheta JM, Rittenhouse PA, Bethea CL, Van de Kar LD (1993) Ibotenic acid lesions in the bed nucleus of the stria terminalis attenuate conditioned stress-induced increases in prolactin, ACTH and corticosterone. *Neuroendocrinology* 57:517-524.
- Grubbs FE (1969) Procedures for detecting outlying observations in samples. *Technometrics* 11:1-21.
- Heal DJ, Prow MR, Buckett WR (1989) Measurement of 3-methoxy-4-hydroxyphenylglycol (MHPG) in mouse brain by H.P.L.C. with electrochemical detection, as an index of noradrenaline utilisation and presynaptic alpha 2-adrenoceptor function. *Br J Pharmacol* 96:547-556.
- Henshall DC (2013) MicroRNAs in the pathophysiology and treatment of status epilepticus. *Frontiers in Molecular Neuroscience* 6:1-11.
- Hioki H, Kameda H, Nakamura H, Okunomiya T, Ohira K, Nakamura K, Kuroda M, Furuta T, Kaneko T (2007) Efficient gene transduction of neurons by lentivirus with enhanced neuron-specific promoters. *Gene Therapy* 14:872-882.
- Howells FM, Russell VA (2008) Glutamate-stimulated release of norepinephrine in hippocampal slices of animal models of attention-deficit/hyperactivity disorder (spontaneously hypertensive rat) and depression/anxiety-like behaviours (Wistar-Kyoto rat). *Brain Res* 1200:107-115.
- Huang CC, Hsu KS, Gean PW (1996) Isoproterenol potentiates synaptic transmission primarily by enhancing presynaptic calcium influx via P- and/or Q-type calcium channels in the rat amygdala. *J Neurosci* 16(3):1026-1033.

- Itoi K, Suda T, Tozawa F, Dobashi I, Ohmori N, Sakai Y, Abe K, Demura H (1994) Microinjection of norepinephrine into the paraventricular nucleus of the hypothalamus stimulates corticotropin-releasing factor gene expression in conscious rats. *Endocrinology* 135(5):2177-2182.
- Johnson M (1998) The β -adrenoceptor. *Am J Respir Crit Care Med* 158:S146-S153.
- Jones BE, Moore RY (1977) Ascending projections of the locus coeruleus in the rat. II. Autoradiographic study. *Brain Res* 127(1):25-53.
- Kita H, Kitai ST (1990) Amygdaloid projections to the frontal cortex and the striatum in the rat. *J Comp Neurol* 298:40-49.
- Kügler S, Kilic E, Bähr M (2003) Human synapsin 1 gene promoter confers highly neuron-specific long-term transgene expression from an adenoviral vector in the adult rat brain depending on the transduced area. *Gene Ther* 10:337-347.
- Krettek JE, Price JL (1978) Amygdaloid projections to subcortical structures within the basal forebrain and brainstem in the rat and cat. *J Comp Neurol* 178(2):225-253.
- Lakner AM, Steuerwald NM, Walling TL, Gosh S, Li E, McKillop IH, Russo MW, Bonkovsky HL, Schrum LW (2012) Inhibitory effects of microRNA 19b in hepatic stellate cell-mediated fibrogenesis. *Hepatology* 56(1):300-310.
- LeDoux J (1998) Fear and the brain: where have we been, and where are we going? *Biol Psychiatry* 44:1229-1238.
- McDonald AJ, (1991) Organization of amygdaloid projections to the prefrontal cortex and associate striatum in the rat. *Neuroscience* 44(1):1-14.
- Neufeld-Cohen A, Tsoory MM, Evans AK, Getselter D, Gil S, Lowry CA, Vale WW, Chen A (2010) A triple *urocortin* knockout mouse model reveals an essential role for urocortins in stress recovery. *Proc Natl Acad Sci USA* 107 (44):19020-19025.
- Palkovitz M, Brownstein M (1988) *Maps and Guide to Microdissection of the Rat Brain*. New York: Elsevier.
- Paré D, Smith Y, Paré J-F (1995) Intra-amygdaloid projections of the basolateral and basomedial nuclei in the cat: *phaseolus vulgaris*-leucoagglutinin anterograde tracing at the light and electron microscope level. *Neuroscience* 69(2):567-583.
- Paré D, Duvarci S (2012) Amygdala microcircuits mediating fear expression and extinction. *Curr Opin Neurobiol* 22:717-723.
- Paxinos G, Franklin KBJ (2001) *The Mouse Brain in Stereotaxic Coordinates*, Second Edition. San Diego, CA: Academic Press.
- Petersen RG (1985) *Design and analysis of experiments*. New York: Marcel Dekker, Inc.
- Pikkarainen M, Ronkko S, Savander V, Insausti R, Pitkänen A (1999) Projections from the lateral, basal, and accessory basal nuclei of the amygdala to the hippocampal formation in rat. *J Comp Neurol* 403:229-260.
- Pitman RK, Orr SP, Shalev AY, Metzger LJ, Mellman TA (1999) Psychophysiological alterations in post-traumatic stress disorder. *Semin Clin Neuropsychiatry* 4(4):234-241.
- Rooszendaal B (2000) 1999 Curt P. Richter Award - Glucocorticoids and the regulation of memory consolidation. *Psychoneuroendocrinology* 25:213-238.
- Roseboom PH, Klein DC (1995) Norepinephrine stimulation of pineal cyclic AMP response element-binding protein phosphorylation: primary role of a beta-adrenergic receptor/cyclic AMP mechanism. *Mol Pharmacol* 47:439-449.
- Russell VA, Wiggins TM (2000) Increased glutamate-stimulated norepinephrine release from prefrontal cortex slices of spontaneously hypertensive rats. *Metab Brain Dis* 15(4):297-304.
- Qu LL, Guo NN and Li BM (2008) β 1- and β 2-adrenoceptors in basolateral nucleus of amygdala and their roles in consolidation of fear memory in rats. *Hippocampus* 18:1131-1139.
- Silberman Y, Ariwodola OJ, Weiner JL (2012) β 1-adrenoceptor activation is required for ethanol enhancement of lateral paracapsular GABAergic synapses in the basolateral amygdala. *J Pharmacol Exp Ther* 343:451-459.
- Staiger JF, Nürnberg F (1991) The efferent connections of the lateral septal nucleus in the guinea pig: projections to the diencephalon and brainstem. *Cell Tissue Res* 264:391-413.
- Sterpenich V, D'Argembeau A, Desseilles M, Balteau E, Albouy G, Vandewalle G, Degueldre C, Luxen A, Collette F, Maquet P (2006) The locus coeruleus is involved in the successful retrieval of emotional memories in humans. *J Neurosci* 26(28):7416-7423.
- Sullivan GM, Apergis J, Gorman JM, LeDoux JE (2003) Rodent doxapram model of panic: behavioral effects and c-Fos immunoreactivity in the amygdala. *Biol Psychiatry* 53:863-870.
- Swanson LW, Cowan WM (1979) The connections of the septal region. *J Comp Neurol* 186(4):621-656.
- Szabadi E (2013) Functional neuroanatomy of the central noradrenergic system. *J Psychopharmacol (Oxf)* 27(8):659-693.
- Takacs PZ, Kotov I, Frank J, O'Connor P, Radeka V, Lawrence DM (2010) PSF and MTF Measurement methods for thick CCD sensor characterization. *Proc Spie* 7742.
- Tanaka M, Yoshida M, Emoto H, Ishii H (2000) Noradrenaline systems in the hypothalamus, amygdala, and locus coeruleus are involved in the provocation of anxiety: basic studies. *Eur J Pharmacol* 405:397-406.
- Tiscornia G, Singer O, Verma IM (2006) Production and purification of lentiviral vectors. *Nature Protocols* 1:241-245.

- Ulrich-Lai YM, Herman JP (2009) Neural regulation of endocrine and autonomic stress responses. *Nat Rev Neurosci* 10:397-409.
- Winter BJ, Brown DR, Michels KM (1991) Design and analysis of factorial experiments: completely randomized experiments. In: *Statistical Principles in Experimental Design*, Third Edition, p342. Boston, MA: McGraw Hill.
- Zhang Z-W, Zhang L-Q, Ding L, Wang F, Sun Y-J, An Y, Zhao Y, Li Y-H, Teng C-B (2011) MicroRNA-19b downregulates insulin 1 through targeting transcription factor neuroD1. *FEBS Lett* 585:2592-2598.

Acknowledgements

This thesis project could not have been completed without the supervision of my graduate student mentor, Evan Paul, and the guidance of my thesis advisor, Dr. Christopher A. Lowry; I would like to extend my most heartfelt thanks to them for their time and attention. I would also like to thank the whole of Dr. Lowry's Behavioral Neuroendocrinology Laboratory for their support and generous sharing of their expertise. I would like to thank the Chen laboratory, namely Dr. Alon Chen and Naama Volk, for their diligent animal work and transgenic expertise, and without whom this manuscript would not have been possible. I would also like to thank the University of Colorado Undergraduate Research Opportunities Program (UROP) and the Biological Sciences Initiative (BSI) for providing funding for this project in the form of two Individual Experimental Research Grants, awarded over the 2013 summer term as well as the 2013-2014 academic year. Additionally, my thanks to Marie Boyko, Senior Instructor in Scientific Writing at the University of Colorado Boulder, for her support, thoughtfulness, and mentorship in my development as a writer, and whose revisions have contributed to the clarity of the final draft of this manuscript. Finally, I would like to thank my thesis committee for their time and consideration: Dr. Christopher A. Lowry, Dr. David Sherwood, and Dr. Robert Spencer.